TURBOMACHINERY & PUMP SYMPOSIA | HOUSTON, TX
SEPTEMBER 15-17, 2020
SHORT COURSES: SEPTEMBER 14, 2020

A REVIEW OF AERODYNAMICALLY INDUCED FORCES ACTING ON CENTRIFUGAL COMPRESSORS, AND RESULTING VIBRATION CHARACTERISTICS OF ROTORS

James M. Sorokes
Principal Engineer
DRESSER-RAND Business,
Part of Siemens Power & Gas
Olean, NY, USA

Mark J. Kuzdzal
Director, Business Development
DRESSER-RAND Business,
Part of Siemens Power & Gas
Olean, NY, USA

James M. "Jim" Sorokes is a Principal Engineer at Dresser-Rand with over 44 years of experience in the turbomachinery industry. Jim joined Dresser-Clark (now the Dresser-Rand business) after graduating from St. Bonaventure University in 1976. He spent 28 years in the Aerodynamics Group, became the Supervisor of Aerodynamics in 1984 and was promoted to Manager of Aero/Thermo Design Engineering in 2001. While in the Aerodynamics Group, his primary responsibilities included the development, design, and analysis of all aerodynamic components of centrifugal compressors. In 2004, Jim was named Manager of Development Engineering whereupon he became involved in all aspects of new product development and product upgrades. In 2005, Jim was promoted to principal engineer responsible for various projects related to compressor development and testing. He is also involved in mentoring and training in aerodynamic design, analysis, and testing.

Jim is a member of ASME and the ASME Turbomachinery Committee. He has authored or co-authored more than fifty technical papers and has instructed seminars and tutorials at Texas A&M and Dresser-Rand. He currently holds five U.S. patents and has several other patents pending. He was elected an ASME Fellow in 2008 and a Dresser-Rand Fellow in 2015. Jim also was given a Lifetime Achievement award by Hydrocarbon Processing magazine in 2019.

Mark J. Kuzdzal is currently the Head of the Advanced Components and Methods group. In this role Mark is responsible for guiding development of the supersonic compression platform, advanced bearing and seal development along with advanced computing and optimization methods. Prior to this assignment he was the Director of Business Development for the supersonic compression platform where he had responsibility for guiding the development team, value proposition, launch activities, and creation of operations, marketing and communication plans to support the supersonic product line.

Prior to this assignment and for nearly a decade, Mark was the Manager of the Core Technologies organization for Dresser-Rand Company. He was responsible for overseeing Rotordynamics, Materials & Welding, Solid Mechanics, Aero/thermo dynamics and Acoustics disciplines.

Mark started his career with Dresser-Rand as a Rotordynamics engineer after earning a B.S. Degree (Mechanical Engineering, 1988) from the State University of New York at Buffalo. Mr. Kuzdzal's areas of expertise focus on rotordynamics, bearing performance, and product/process development. He has co-authored numerous technical papers and holds many U.S. Patents. Mr. Kuzdzal is an emeritus member of the Texas A&M turbomachinery advisory committee and the Penn State Behrend Mechanical Engineering Technology industrial advisory committee. He is a NLA and ASME member.

ABSTRACT

There are several sources of non-synchronous forced vibration of centrifugal compressor rotors. Many of them are aerodynamic phenomena, created within the gas path of the compressor. Phenomena such as impeller stall, diffuser stall (with and without vanes), and flow instabilities caused by impeller to diffuser misalignment, are all characteristic flow disturbances that can cause forced vibration. In fact, often the only indications of these phenomena are found in the resulting rotor vibration signals.

Several phenomena that can cause non-synchronous vibration are reviewed, and for each one, background information, as well as detailed descriptions of the flow field, or other source of the excitation, is provided. This includes the use of CFD analytical results to describe the flow where applicable.

The review also includes, when available, dynamic pressure transducer test data that can be used to verify the presence of the phenomena, and rotor vibration data indicating the presence of such phenomena. This includes test data of actual machines, indicating characteristics such as frequency and amplitude.

INTRODUCTION

This discussion centers on forced vibration of rotors, the sources and reasons for the forces involved, and the resulting vibration characteristics as might be revealed by non-contacting rotor probes. To adequately cover this information, we must start with a basic description of rotor vibration characteristics, and the response of rotors to various types of excitation. Once this is complete, our discussion will move on to descriptions of the causes of each of the phenomenon of interest, and then to the resulting vibration signals.

Fortunately, the primary rotor vibration characteristics of interest can generally be illustrated by reference to simple models. This allows us to describe them without resorting to involved differential equations and their solutions. The description of the causes of the forcing phenomena is much more specific to centrifugal compressors, as opposed to rotors in general. Here, the forces that can be generated within the gas path are described, and the reasons for those forces are covered in detail. In some cases there is data available regarding the dynamic pressure fields created by these phenomena, and where it is available, it has been included.

The resulting rotor vibration signals are the primary way we can become aware of these forcing functions. With an understanding of how rotors respond to forces, and the potential forcing functions they may encounter, the recognition of vibration due to such phenomena becomes simpler than it otherwise may be.

VIBRATION CHARACTERISTICS

As noted above, we are fortunate that the vibration characteristics of interest can be described using simple one degree of freedom systems. The material below describing those characteristics could be extracted from most vibration texts, such as those listed in the bibliography. It has simply been condensed and described in a manner that is most relevant to the particular problem of rotors.

Free Vibration

Free Vibration Without Damping - For our purposes, the simple spring-mass system, as depicted in Figure 1, can be used for much of our discussion of the features of interest for a rotor system undergoing free vibration. Equation (1), the equation of motion for this simple system, produces the general solution defined by Equation (2).

$$m\ddot{x} + kx = 0 \qquad (1)$$

$$x = X\sin(\omega_n t + \Phi) \qquad (2)$$

$$\omega_n^2 = k/m \qquad (3)$$

Where:

m = mass
$\ddot{x}$ = acceleration
k = spring coefficient
x = position/amplitude
X = maximum position/amplitude
ω_n = natural frequency
t = time
Φ = phase angle

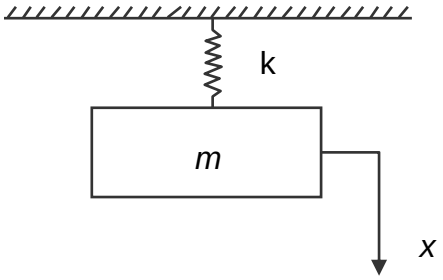

Figure 1. Simple Spring-Mass System.

In the absence of damping or external forces, once such a system is moved from its equilibrium position, the vibration as described by the equations continues forever, at the harmonic frequency defined by Equation (3).

Free Vibration With Damping - The situation can both be complicated slightly, and made much more realistic, by adding (viscous) damping. For the purposes of this discussion, the simple one degree of freedom spring-mass-damper system, as depicted in Figure 2, can be used to describe the features of interest for a rotor system with damping undergoing free vibration. Equation (4) is the equation of motion for this simple system.

$$m\ddot{x} + c\dot{x} + kx = 0 \qquad (4)$$

$$C_{cr} = 2\sqrt{\mathrm{km}} \qquad (5)$$

$$x = Xe^{-\mu t}\cos(pt + \Phi) \qquad (6)$$

Where, in addition to the definitions above:

c	= damping coefficient
$\dot{x}$	= velocity
C_{cr}	= critical damping
p	= as defined below
μ	= as defined below

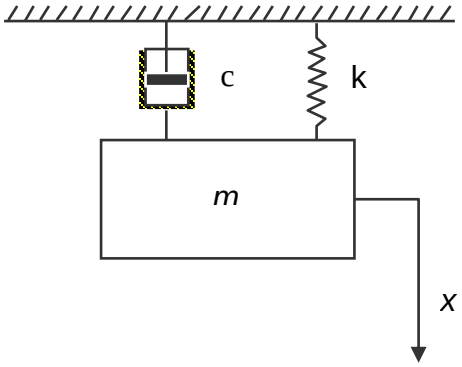

Figure 2. Simple spring-mass-damper system.

If critical damping is defined by Equation (5), and we investigate only the case where damping is less than critical, then a solution is generated as defined by Equation (6). This solution has a harmonic component $\left(\cos(pt + \Phi)\right)$ with a natural frequency given by $\left(pt,\ where\ p = \sqrt{\omega_n^2 - \mu^2}\ and\ \mu = \frac{c}{2m}\right)$, and a decaying component $\left(e^{-\mu t}\right)$, with the rate of decay determined by the coefficient in the exponent $\left(\mu\right)$. With any given initial position not at the equilibrium position of the system, the value of this

exponent determines the rate at which the vibration of the system will return to zero. The coefficient over one period of vibration ($\mu T, \quad where \;\; T \; is \;\; one \;\; period$) is called the logarithmic decrement (log dec), and it is defined by Equation (7).

$$\delta = \mu T \qquad (7)$$

It is, therefore, evident that whether or not there is any damping in the system, the system in free (unforced) motion will vibrate only at its natural frequency. The amplitude is completely defined by the motion at the natural frequency, and if damping is present, the log decrement defines the rate of decay.

Forced Vibration

While there are several types of forces that can act on compressor rotors, they all can be characterized as either periodic or non-periodic (arbitrary). First we will discuss harmonic forces, a subset of periodic forces. The more general case of periodic forces is then covered, followed by arbitrary forces.

Harmonic External Forces

These types of forces can be represented by a simple sine wave. The force is of the form shown in equation (8), and results in an equation of motion for a damped single degree of freedom system as shown in equation (9). We get a general solution of the form in equation (10). As shown by equation (11), for a given relative force level $\left(D = F/k \right)$ the amplitude is dependent on the relative location of the forcing function frequency to the system natural frequency $\left(\tau = \omega/\omega_N \right)$, as well as the amount of damping in the system $\left(\rho = \frac{c}{2m\omega_n} \right)$. As equation (10) shows, the frequency of the vibration is at the frequency of the forcing function, not the system natural frequency. At low levels of damping, it is also apparent from equations (10) and (11) that the amplitude response to the force would approach infinity as the forcing function frequency approaches the system natural frequency. This is the familiar concept of resonance.

$$s(t) = F\cos(\omega t) \qquad (8)$$

$$m\ddot{x} + c\dot{x} + kx = F\cos(\omega t) \qquad (9)$$

$$x = P\cos(\omega t - \Phi) \qquad (10)$$

$$P = \frac{D}{\left[(1-\tau^2)^2 + (2\rho\tau)^2\right]^{1/2}} \qquad (11)$$

Where, in addition to the earlier definitions:

$s(t)$ = harmonic forcing function

ω = forcing function frequency

F = maximum of forcing function

P = maximum of response amplitude

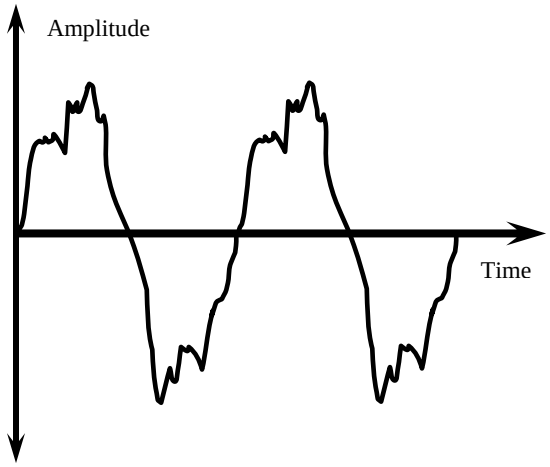

Figure 3. Periodic Signal.

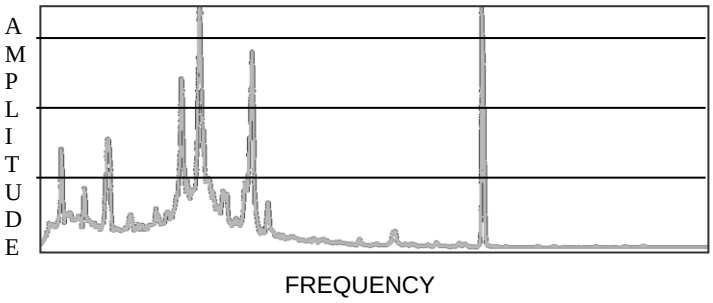

Figure 4. Frequency spectrum from periodic vibration signal.

It is therefore evident that the steady state response of a system to a harmonic forcing function is harmonic motion at the same frequency as the force, with maximum amplitude occurring when the system natural frequency is in resonance with the forcing function.

Periodic External Forces

A periodic force is not a clean sine wave, but it does repeat itself over some time period, with a frequency of ω. In that case, the forcing function may be expanded in a Fourier Series, and the force is described in the form of equation (12). Any periodic signal can be expanded in this way, and we use this capability every time we look at vibration spectrum data. It is this characteristic that allows an FFT (Fast Fourier Transform) Analyzer to translate a vibration signal such as that shown in Figure 3 into the frequency domain, as in Figure 4.

$$s(t) = \sum_{1}^{\infty} F_n \cos(n\omega t + \theta_n) \quad (12)$$

$$x = \sum_{1}^{\theta} P_n \cos(n\omega t + \theta_n - \phi_n) \quad (13)$$

$$P_n = \frac{D_n}{\left[(1-n^2\tau^2)^2 + (2\rho n\tau)^2\right]^{1/2}} \quad (14)$$

Where, in addition to the earlier definitions:

F_n = the nth multiple of the force
n = the nth multiple
θ_n = the phase angle related to the nth multiple force
P_n = the maximum of the nth multiple position/amplitude
ϕ_n = the phase angle related to the nth multiple amplitude
D_n = the relative force level of the nth multiple

The steady state response of a simple spring-mass system to a force in the form of equation (12) is shown by equation (13). This indicates the vibration occurs at the frequency of the forcing function and its multiples (often called harmonics, and not to be confused with the harmonic forcing function mentioned above). As shown by equation (14), the amplitude is maximized when the base forcing function frequency, or any of its multiples, equals the system natural frequency. It is then apparent that the response of a system to a periodic external force can be analyzed by decomposing the forcing function into its components (Fourier Series), and then analyzing the response of the system to each of those components. The total response of the system is given by the sum of the individual responses, which can be looked at as harmonic forces, as described earlier.

Arbitrary, or Non-periodic, External Forces

These types of forces are transient in nature, and the most common way to investigate them is to consider an impulse force. An impulse is typically a force of significant magnitude that acts for a short but finite time, and can be represented by an equation of the form in equation (15). When a simple spring mass system is excited by such an impulse, it responds in free vibration with initial conditions of $(x = 0)$ and $(\dot{x} = {}^{F}/_{m})$. This results in vibration as represented by equation (16), which can be seen to be at the system natural frequency, with an amplitude linearly related to the magnitude of f.

$$f = \int_{t}^{t+\varepsilon} F dt \qquad (15)$$

$$x = \frac{f}{m\omega_n} \sin \omega_n t = f\, g(t) \qquad (16)$$

Where, in addition to the earlier definitions:

f = the unit impulse force

F = the impulse force amplitude

$g(t)$ = response to the unit impulse force

Using the principle of superposition, excitation due to arbitrary external forces, as depicted in Figure 5, can be treated as a series of impulses. The resulting response is defined by a superposition integral, in the form of equation (17).

$$x = \int_{0}^{t} f(t')g(t-t')dt' \qquad (17)$$

This means the general response of the system would be expected to be movement due to the forces themselves, plus vibration at a natural frequency, with varying amplitude levels, depending on the timing of the impulses. The relationship of any new impulse force to the existing vibration would determine the resulting vibration.

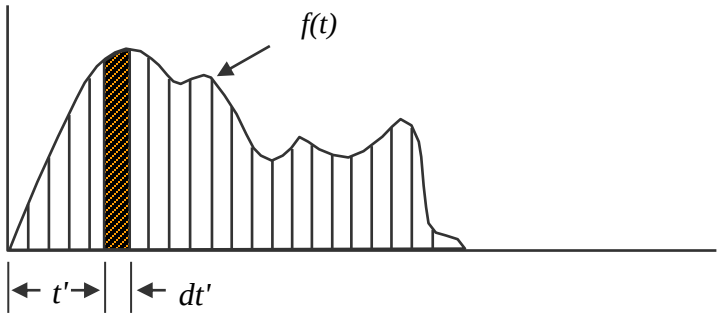

Figure 5. Force due to series of impulses.

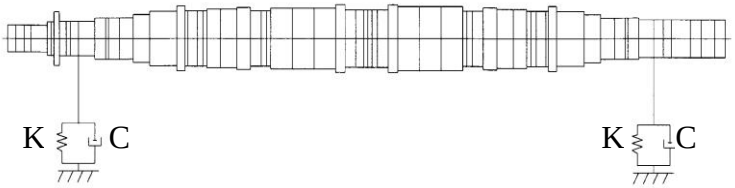

Figure 6. Rotor system model.

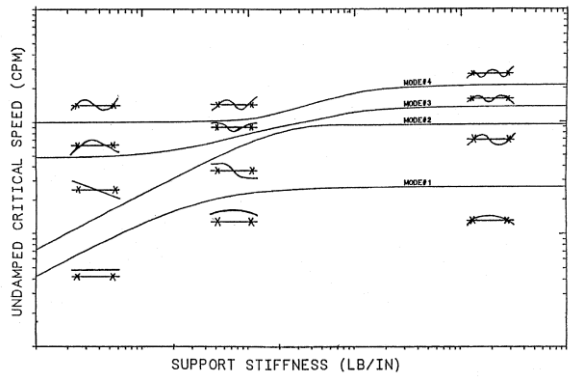

Figure 7. Critical speed map.

Summary

The above description points out an important distinction between different types of forced vibration. Purely harmonic forcing functions will result in vibration at the frequency of the force, with the amplitude depending on the level of force and the proximity of the forcing frequency to the system natural frequency. The more general form of periodic forcing functions will result in vibration at the frequency of the force, plus its multiples, with the amplitude again dependent on the level of the force, plus the proximity of the forcing frequency, or any of its multiples, to the system natural frequency. In contrast, vibration due to a non-periodic, or arbitrary forcing function, will occur at the system natural frequency. The amplitude at that frequency will vary, and other movement in response to the forces will appear as random amplitudes and frequencies in the spectrum.

APPLICATION TO ROTOR VIBRATION

A compressor rotor can be considered as a special type of multi degree of freedom system. As such, it can exhibit both free vibration and forced vibration. Free vibration takes place when the system vibrates due to forces inherent in the system itself. This vibration always takes place at one or more of the natural frequencies of the system. Forced vibration occurs due to external forces. If this force is periodic, as it often is, the system will vibrate at some combination of the frequency of excitation and its multiples, with amplitudes dependent on the position of the excitation frequencies to the system natural frequencies. For non-periodic forces, the response of the system will again be at some combination of its natural frequencies.

The following should illustrate these characteristics in more detail.

Free Vibration

Free Vibration without damping

If we have a multi degree of freedom system, such as a compressor rotor, the above basic principles still apply. The system is more complicated, but has the same basic components. For calculation purposes, the mass is represented by the modeled rotor stations, and the spring is represented by stiffness matrices between mass stations on the rotor, and by stiffness coefficients at the bearing locations. A typical rotor system model for an undamped model of this type might look like Figure 6 without the damping (C).

For each degree of freedom in this model, there will be an (undamped) natural frequency. Such a model can therefore be used to generate the familiar critical speed map, as shown in Figure 7, where these frequencies vary with the spring coefficient applied at the bearing location. Each of these natural frequencies also has a mode shape. These describe the way the rotor vibrates when at the particular natural frequency in question. The first four of these mode shapes for a typical beam style compressor would be as depicted in Figure 7. The result is a rotor system that has multiple natural frequencies, or principal modes. When undergoing free vibration, the overall vibration of the system is always some superimposed combination of these modes.

Free Vibration with damping

Again, in a multi degree of freedom system, such as a compressor rotor, the basic principles discussed above still apply. With damping, the system becomes more complicated, but still has the same basic components. For calculation purposes, the rotor is represented by the modeled rotor stations, with the spring and damper represented by stiffness and damping coefficient matrices at any bearing and seal locations. A typical rotor system model might look like the one in Figure 6 but spring and damping coefficients in multiple directions are considered at each bearing, seal or other support point, as shown in Figure 8.

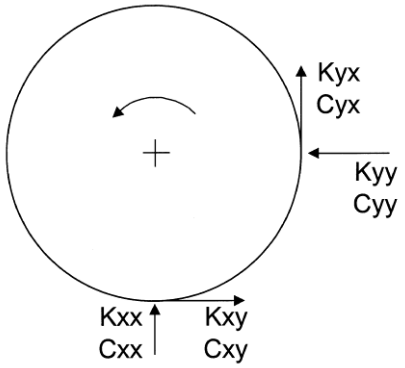

Figure 8. Cross coupling coefficients.

For each degree of freedom in this system, there will be a damped natural frequency, often called an eigenvalue, again with a corresponding specific mode shape, and also with a logarithmic decrement. Each eigenvalue has its own decay rate, as defined by the log dec, which can therefore be used as a measure of available damping. The result is a rotor system that has multiple natural frequencies (eigenvalues), each of them having a specific mode shape and an amount of damping indicated by the log dec. Just as in the undamped case, the overall free vibration of this system will always be some combination of all the natural frequencies, and therefore of all the mode shapes.

Since, in the absence of any external forcing function, the vibration of a system such as a rotor can only occur at its natural frequencies, the dominant frequency of any vibration signal must be one of these natural frequencies. The result is a very clean vibration signal at typically one of these frequencies, with an amplitude that can be substantial.

In the real world, the situation most closely resembling such free vibration is rotor instability, where a mode (typically the first or fundamental) is caused only by the "passive" excitation, represented by the spring and damping coefficients shown in Figure 8. This same figure can also be used to illustrate that "cross-coupling" coefficients (such as k_{xy}) can drive the rotor in a whirling motion.

Analytical techniques used to examine rotor stability can create an "unstable" rotor model mathematically simply with these coefficients at the bearing and seal locations. External forces are not needed. The term passive is used because forces are only

generated in response to movement of the rotor, creating a self-generating mechanism. The term instability is used because with the right coefficients, the log dec of the mode of interest can go to zero, or below, creating an unstable situation, with constantly increasing amplitude. The vibration is unbounded, until nonlinearity takes over (often as in contacting the bearing or seal).

The characteristics of rotor "instability" are therefore a clean, single frequency signal, occurring at the rotor natural frequency, with an amplitude that increases until bounded by other constraints. This type of subsynchronous vibration can be a serious problem. It can cause severe damage. Fortunately, it is not as commonplace as it once was. There are other reasons for compressors to vibrate at subsynchronous frequencies, however, and that is the primary topic of the rest of this discussion.

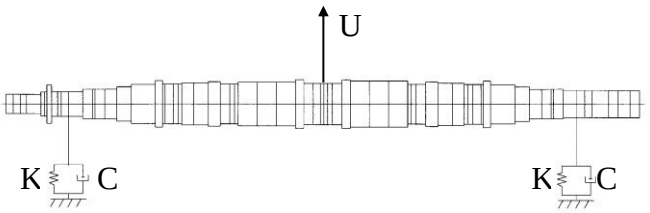

Figure 9. Rotor system model showing unbalance force.

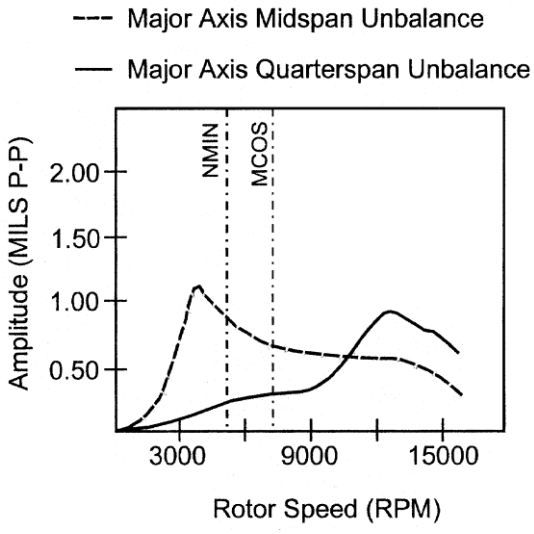

Figure 10. Amplitude versus speed plot.

Forced Vibration

Harmonic Forces

An obvious instance of a harmonic force on a rotor is unbalance. For analysis, the rotor model adds a rotating force, as shown Figure 9. Its frequency is obviously equal to running speed, and we can produce the familiar amplitude v. speed plots, as shown in Figure 10, to measure response of the rotor to this external force. Since we are dealing with a multiple degree of freedom system, the vibration mode shape will vary depending both on how close the speed (forcing function frequency) is to the various natural frequencies, and the location of the unbalance. The location used for measuring vibration introduces another variable, since the mode shape at any given frequency will determine whether a particular probe location can be used to adequately measure response of the rotor. Similarly, asynchronous response analysis of a rotor to reduced frequency excitation can provide some picture of a rotor's ability to withstand a specific subsynchronous harmonic force.

A vibration signal due to a consistent harmonic external force would therefore be expected to be a steady vibration, with an amplitude dependent on the force and the proximity to a rotor natural frequency. This characteristic would result in a resonance at each natural frequency that becomes coincident with the force. If the frequency of a subsynchronous force changes, the vibration response frequency will also change, with the amplitude rising and falling depending on the proximity to the natural frequencies of the rotor. For a given system, with a given forcing function, we therefore have a relatively stable situation, with essentially no tendency to exhibit sporadic high vibration levels.

Periodic Forces

Non-synchronous forces acting on rotors are generally in the form of aerodynamic forces. When these aerodynamic forces are periodic, they may or may not be harmonic, as well. A response plot similar to Figure 10 could again be used to examine the asynchronous response of the rotor to the force, or any multiples it may have. From the discussion above on periodic forcing functions, it is apparent that at frequencies below a given natural frequency of the system, both the force and any of its multiples can excite that mode if they are either in resonance, or close to resonance, with the natural frequency. On the other hand, periodic forces at higher frequencies cannot be in resonance with lower natural frequencies.

Just as for a single degree of freedom system, any vibration due to such forces will be at frequencies equal to the forcing function frequency, plus any integer multiples. The amplitude will vary as the frequency varies, depending on the proximity of the frequencies to rotor natural frequencies, and resonance can occur with any of the natural frequencies and the forcing function or any of its multiples. Again, for a given system under given conditions, this type of vibration is stable, consistent and repeatable.

Arbitrary Forces

Arbitrary external forcing functions seen by compressor rotors are generally caused by transient aerodynamic activity. Since they act as an impulse force, however, they may also cause vibration at frequencies other than one of the rotor's natural frequencies. However, the reaction of a rotor to aerodynamic activity that can cause transient arbitrary forces is not generally analyzed, since the potential characteristics and locations of the forces involved are innumerable. It is then left to evaluation of vibration signals to determine potential causes of vibration, and whether they should cause any concerns.

Just as with a single degree of freedom system, arbitrary forcing functions can cause vibration at one or more of a rotor's natural frequencies. The amplitude at the natural frequency will vary, however, as the amplitudes of the various impulses vary. Other movement of the rotor due to the impulse forces would appear as random frequencies and amplitudes on a signal analyzer. Steady vibration at any frequency will not occur, however. This type of forced vibration can therefore be separated from unforced "instability" when evaluating vibration data most readily by viewing real time signals, to separate relatively steady or constantly increasing vibration from unsteady vibration at multiple frequencies. In real time, amplitudes and frequencies will constantly vary, with natural frequencies being the most prominent in most instances. Vibration levels will be determined by the stiffness and damping of the system, and the amplitude of the forces applied.

We can see from these results that unforced subsynchronous vibration (instability) will be a relatively clean signal at the rotor natural frequency. Forced subsynchronous vibration due to an harmonic force will be a clean single frequency that is often not at a rotor natural frequency. Forced subsynchronous vibration due to a periodic force will be at a frequency and its multiples, again usually not at a rotor natural frequency (although the existence of multiples increases the chance of resonance). Finally, forced subsynchronous vibration due to arbitrary (impulse) forces will be at multiple, and continuously varying frequencies and amplitudes, with maximum amplitudes usually occurring near rotor natural frequencies. With this basis, it is useful to describe the causes of some of the harmonic, periodic and arbitrary forces that can create such vibration signals.

AERODYNAMIC FORCES

Definitions

Before further discussions on the aerodynamic forces, a definition of four terms must be presented so that there is no confusion as to their interpretation in this document. Those terms are surge, stall, rotating stall, and hysteresis zone and they are defined as follows:

Surge - is a system phenomenon that is not only dependent on the compressor but on all components of the process; i.e., piping, valves, pressure vessels, volumes, etc. Surge is defined as an operating condition at which full flow reversal occurs; i.e., flow progresses backward through the compressor section or stage and comes out the inlet. [Note, it is possible for one stage within a compression section to surge without the entire section surging.] It is typically accompanied by high radial and axial vibrations as well as extreme fluctuations in inlet and discharge pressure and temperature.

Stall - A more localized phenomenon than surge, stall occurs when there is a localized region of reverse flow, reduced velocity/momentum, depressed pressure, etc. Stall can occur within a component of a stage and is frequently accompanied by an increase in subsynchronous vibration as well as pressure pulsations and a possible reduction in stage pressure rise. It is important to note that stall can occur at any point on a compressor operating map but is more common at very high or very low flow rates.

Rotating stall - refers to that class of stall cells which rotate about the compressor; typically in the circumferential direction. The term is borrowed from the axial compressor world where it referred to the progression of a stall cell (or cells) from one rotor passage to the

next. In the centrifugal world, it encompasses any stall cells which move relative to the stationary frame of reference. However, it is most commonly associated with impellers or diffusers.

Hysteresis Zone - When reducing flow, a phenomenon will appear at some flow rate. The phenomenon does not disappear simply by moving back above that flow rate. Instead, the flow rate has to be increased significantly beyond the onset rate to "wash out" the stall cells (Figure 11).

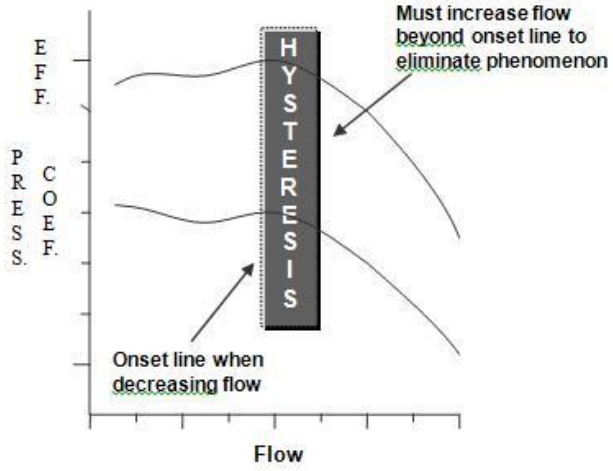

Figure 11. Hysteresis Zone.

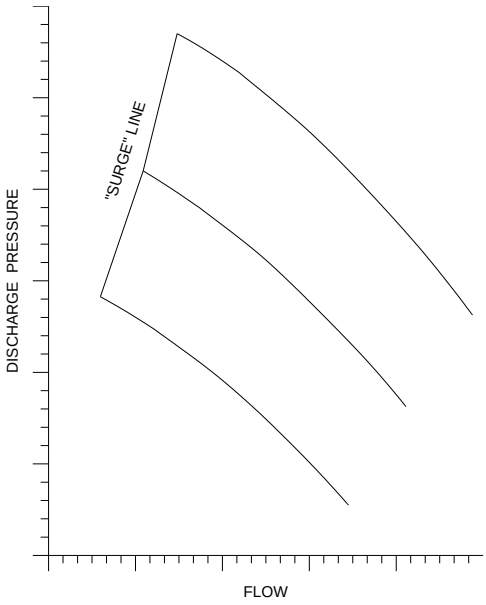

Figure 12. Compressor map showing "surge" line.

It is important to understand the distinction between surge and stall (or rotating stall). Quite often, turbomachinery engineers and users misinterpret or misuse these terms, leading to confusion as to which of the phenomena are happening in a compressor. Much of the confusion occurs because of the common practice of labeling a compressor's minimum stable flow rate as the "surge line" (Figure 12). In fact, the minimum flow rate shown on most as-tested performance maps is dictated by stall rather than surge. Stall or rotating stall tends to be a precursor to true surge. That is, as the inlet flow is reduced, the compressor will experience stall before it encounters a full flow reversal or surge. In some compression systems, the flow increment between the onset of stall and the onset of true surge is very small and it may be impossible to detect the stall without encountering full surge. In other systems, there is a significant difference in the flow rates at which stall and surge occur.

It should also be noted that the vibration signatures resulting from surge and rotating stall are quite different due in part to the amount of flow associated with the two phenomena. As noted, stall and/or rotating stall are localized phenomena so there is a limited amount of flow involved while surge, being a total system phenomenon, involved large amounts of flow. Given the larger amount of flow and

the time required to change direction or momentum, the frequencies associated with surge are typically lower than those associated with rotating stall.

No further commentary will be offered on the system phenomenon, surge. Rather, the discussion will center on stall and, in particular, impeller and vaneless diffuser rotating stall.

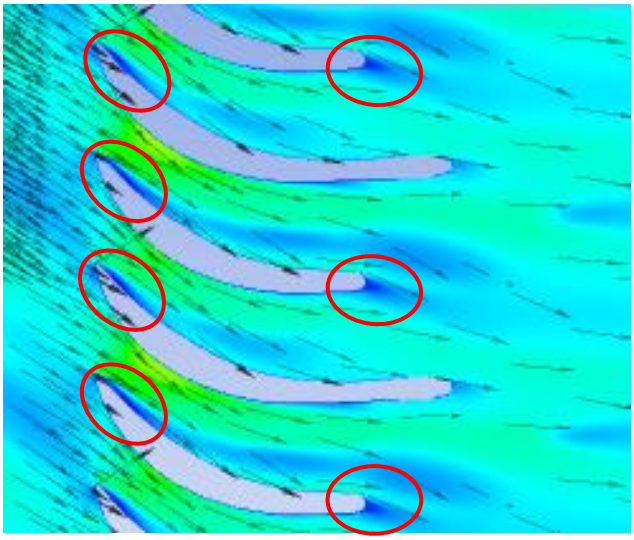

Figure 13. Stationary stall cell in a return channel.

Stationary Stall

Before addressing rotating stall, a few comments are warranted on the stationary form. Stationary stall cells may or may not have detrimental effects on compressor aerodynamic and mechanical performance. Much like its rotating counterpart, stationary stall causes non-uniform pressure fields or unbalanced forces which can influence the compressor rotor. Stationary stall cells can form in vaned diffusers, return channels, guide vanes, near volute tongues, etc. The most common factor which promotes the formation of stationary stalls is high levels of incidence (i.e., the difference between the gas approach angle and the vane setting angle -- Figure 13). High incidence occurs as a compressor or compressor stage is operated far from its nominal or design flow condition; that is, near surge or in overload. The separation cells create pressure disturbances which influence other upstream or downstream stage components. For example, the impeller shown in Figure 14 would be affected by the non-uniform pressure field caused by the flow separation from the diffuser vanes. The interaction of the impeller with this non-uniform field may be evidenced by an increase in vibration at blade-vane passing. Obviously, diffuser vane angles must be set accurately to insure that high incidence and the resulting separation will not arise within the compressor's required operating map.

Stationary stall formation can also occur when flow encounters very tight curvatures. If curvature radii are too small in a return bend, guidevane, on a return channel vane, etc., the flow separates from the highly curved surface and a stall cell can form. Misalignment of parts in a compressor flow path can also cause the flow to separate or stall. All of these phenomena might induce rotor vibrations or contribute to such by prompting the formation of rotating stall. For example, if stationary stall cells form in a return channel or guidevane passage, the stall may disturb the flow field such that rotating stall would initiate in the downstream impeller. Therefore, stationary stall cannot be totally ignored as a possible contributor to rotor excitation. However, no further comments will be offered on the subject.

Rotating Stall

Rotating stall is best described as a non-uniform circumferential pressure field which rotates at a speed other than the compressor operating speed. The non-uniform pressure field might exert unbalanced forces on the compressor rotor, sometimes resulting in asynchronous vibrations. Since the rotational speed of the pressure field is most often lower than the rotor rotational speed, the vibration frequencies are subsynchronous.
As noted, the two most common forms are impeller and diffuser rotating stall. Both may have significant effects on mechanical and aerodynamic performance. In most compressors, rotating stall does not appear except at lower flow rates; i.e., very near surge. However, in some cases, they have been encountered very near design flow. Further complicating matters, some forms of "interaction stall" actually are more prevalent at the high capacity end of the performance map.

Confounding the situation even further, other components can produce forces that affect the rotor vibration signatures, approximating stall characteristics; i.e., seals and bearings. However, these rotor effects are typically not as sensitive to compressor operating conditions. Their response frequency is normally evident over the entire operating envelope and remains relatively constant despite changes in flow rate or discharge pressure. Of course, compressors containing honeycomb or other types of damper seals can exhibit changes in the rotor amplitude and frequency at different pressure levels due to the damping and/or stiffness added to the system. However, rotor-related phenomena will not adhere to all of the characteristics exhibited by aero-related phenomena. It is important to rule out such effects before attributing a subsynchronous rotor vibration to rotating stall.

IMPELLER ROTATING STALL

Numerous researchers have investigated impeller rotating stall and there are equally numerous amount of theories and opinions as to its nature and influences on compressor aero-mechanical performance. Much of this work was drawn from or based upon studies done in the axial compressor world. However, the two early works that gained some notoriety in the centrifugal fraternity were those of Abdelhamid (1980) and Frigne/Van den Braembussche (1984). Their efforts sought to classify the various forms of rotating stall that could occur in a centrifugal stage.

Abdelhamid suggested that impeller rotating stall could result from flow perturbations at the impeller exit that would not allow the flow to follow the blading. These perturbations may be a consequence of disturbances within the impeller passages (i.e., separation cells -- Figure 14) or strong interactions between the impeller and the diffuser (i.e., the diffuser walls interfering with the impeller exit area through misalignment of parts, etc.).

Frigne and Van den Braembussche also studied the characteristics of rotating stall (impeller and diffuser) and published a series of criteria that have been widely used to distinguish between the various types. Their study identified two distinct forms of impeller stall; abrupt and progressive. They also felt that the abrupt stall was the result of strong interactions between the impeller and diffuser while the progressive variety was more the consequence of the impeller flowfield itself. Their publication identified the frequency range for the two types as follows: Abrupt - 26% to 31% of running speed; Progressive - 67% to 82% of running speed.

Other researchers have identified the probable causes for progressive impeller rotating stall as: a) flow separations near the impeller exit; b) incidence angles at the impeller leading edge; or c) pressure disturbances caused by the impeller blade geometry. Based on a review of their published works, impeller rotating stall can manifest itself as frequencies from 26% of running speed up to 100% of running speed. It has also been suggested that some investigators confused diffuser stall as impeller stall. In short, though much has been published on the subject of impeller rotating stall and though many claim to have complete knowledge on the issue, the inconsistencies and contradictory nature of their guidelines, observations, and/or conclusions suggest that additional work is required before anyone can claim a total understanding of this phenomenon.

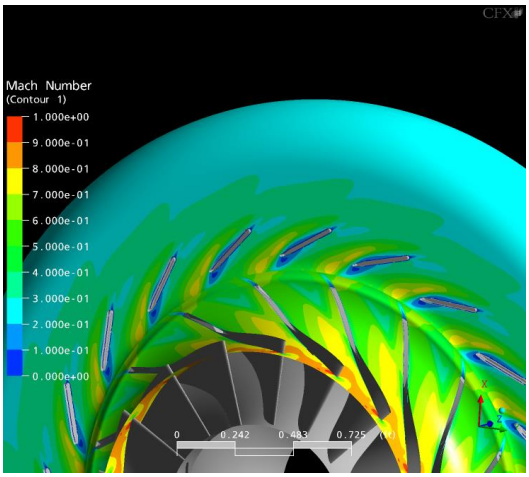

Figure 14. Flow separation in impeller due to interaction with separated diffuser.

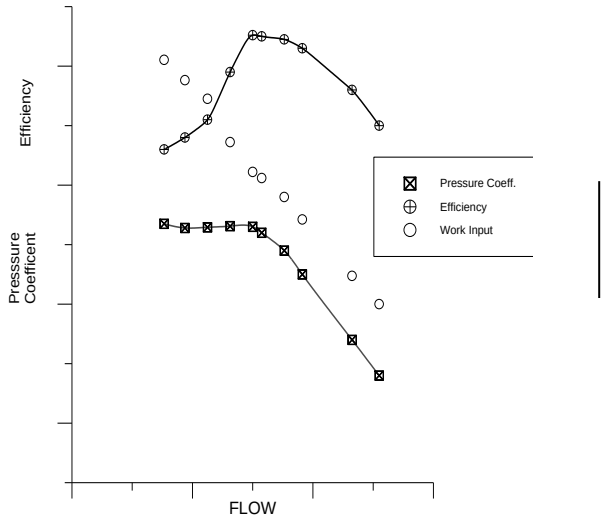

Figure 15. Data from compressor stage experiencing impeller stall.

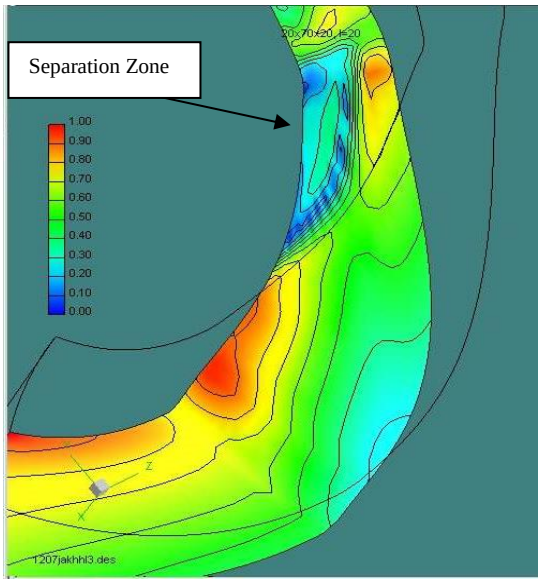

Figure 16. Impeller CFD analysis showing separation zone.

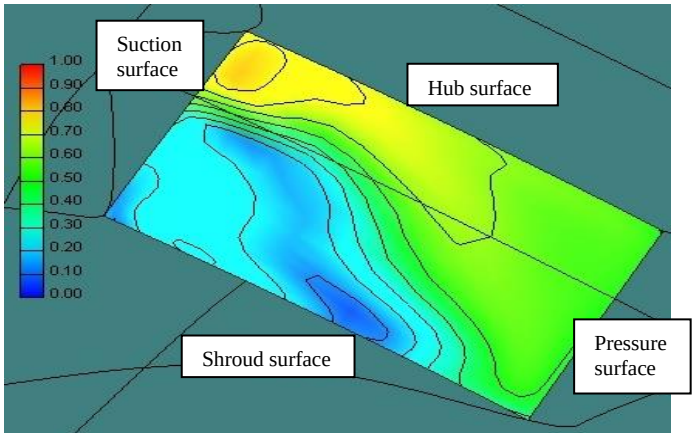

Figure 17. Impeller exit Mach number distribution.

Impeller Rotating Stall Characteristics

Compressors experiencing impeller rotating stall can exhibit some or all of the following characteristics:

- The subsynchronous radial vibration frequency falls in the range of from 50% to 80% of the compressor running speed. NOTE: as suggested above, this range could be as large as from 26% to 100% of running, though the smaller range is more widely accepted.
- The subsynchronous vibration frequency tracks with running speed.
- There is normally no hysteresis zone associated with impeller stall. That is, there will be a very distinct flow rate at which the problem will come and go.
- It may be possible to throttle through the indications of stall such as subsynchronous vibration. That is, it may only occur over a limited flow band and disappear at lower flow rates. For example, when reducing flow rate, a subsynchronous vibration due to such a stall may arise at some Q/N. The vibration persists with further reduction in flow until a point is reached where it disappears.
- There may be a discontinuity or "droop" in the performance curve associated with the onset of the subsynchronous vibration.

Unfortunately, as noted, there is no consensus on the characteristics of impeller rotating stall. As such, it is difficult to provide definitive guidelines for its identification. However, there is good agreement on the various contributors to impeller stall; that is, geometric configurations or flow profiles to avoid. All also agree that detailed 2-D or 3-D analyses of the impeller and its associated hardware can identify potential sources for impeller rotating stall. However, how such stalls manifest themselves (i.e., characteristic frequencies) is still the subject of much debate.

Examples of Rotating Stall Attributed to Impellers

In the past, high flow coefficient stages have been more susceptible to impeller rotating stall. Some obsolete high flow impellers have shown a drooping trend in the pressure coefficient curve in the region between design and surge flow, especially when applied at high tip Mach number, U2/A0 (Figure 15). This droop was accompanied by an increase in subsynchronous vibration at approximately 66% of the compressor running speed. Note that this frequency falls within the guidelines for impeller stall published by Frigne and Van den Braembussche (1984). Also, the general shape of the performance curve for these impellers agreed with the trends observed by the two researchers.

One-dimensional analyses on these obsolete impellers showed no obvious problems; i.e., relative velocity ratios, incidence levels, and various other parameters gave no indications that these impellers would suffer stall problems. Two-dimensional studies also yielded satisfactory results, i.e., loading parameters and velocity distributions fell within the generally accepted guidelines. However, when 3-D flow field analyses (CFD) were performed, some clear shortcomings were observed.

CFD analyses showed that large separation zones were forming in the impeller passages, prompted by high levels of turning both along the shroud and on the blading (Figure 16). These separation zones were coalescing into large wake regions at the impeller exit and applying an excitation force to the rotor (Figure 17). Redesign of the impellers to an arbitrary bladed, full inducer configuration eliminated the stall and all related performance problems. These results were reported by Sorokes and Welch (1991) and Sorokes (1993). In light of the problems with these impellers, new guidelines to limit the amount of blade and cover turning were implemented.

In the late 1990s, a novel form of impeller stall was experienced during full-load, full-pressure testing on a barrel compressor for high pressure gas re-injection. The unit exhibited subsynchronous radial vibration at 91% of running. Of significance, the subsynchronous only became apparent during the full-load, full-pressure testing. There was no indication of any vibration problems during the class III test; i.e., performed at reduced pressure, gas density, and horsepower. Adding to the peculiarity, the subsynchronous vibration only occurred when the second section of the compressor was operating in a very limited flow range (Figure 18). Also, there was absolutely no evidence of a problem in the performance of the compressor; that is, there was no discontinuity in the efficiency curve or head coefficient rise throughout the flow band in which the subsynchronous vibration occurred. It is important to note that all of the impellers, diffusers, return channels, etc. had been used in numerous previous applications without incident. Further, 1-D reviews had been conducted on all impellers and diffusers to insure that they conformed to the guidelines for rotating stall avoidance that were being applied at the time. In short, there was no reason to suspect a rotating stall problem.

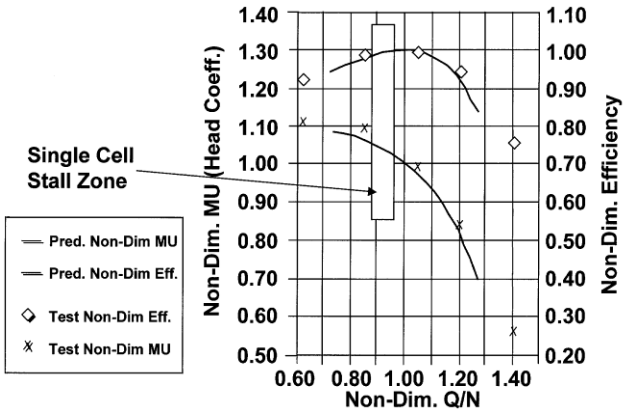

Figure 18. Performance map showing apparent impeller stall zone.

To identify the source of the excitation, dynamic pressure probes were installed in the diffusers and second section inlet. During the testing, pressure pulsations were discovered in the first and second stages of the second section that coincided with the onset of the subsynchronous radial vibration detected by the vibration probes (Figure 19). When throttling the compressor from design to lower flow rates, the pressure pulsations initiated at a frequency of 91% of running; i.e., exactly the same as the subsynchronous radial vibration frequency. With further reduction in flow rate, the pressure pulsation frequency changed to 182% of running speed. Coincident with this pulsation frequency change as seen in the pressure signals in Figure 20, the subsynchronous radial vibrations disappeared. With even further decreases in flow rate, the pressure pulsation frequency changed to 273% of running and then 364% of running, yet the subsynchronous radial vibrations never returned.

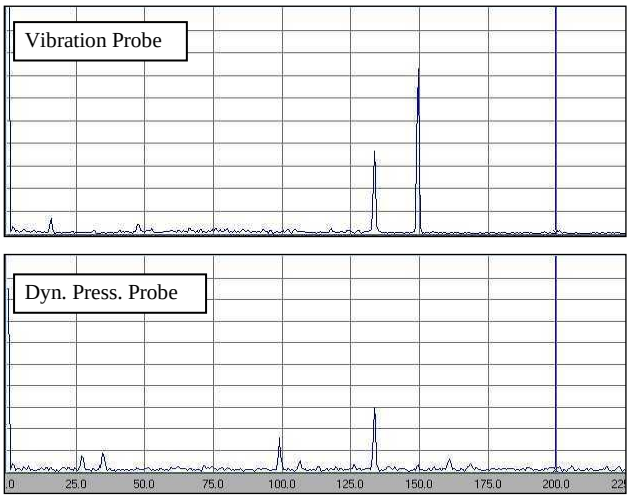

Figure 19. Spectra from dynamic pressure probe and vibration probe during impeller rotating stall.

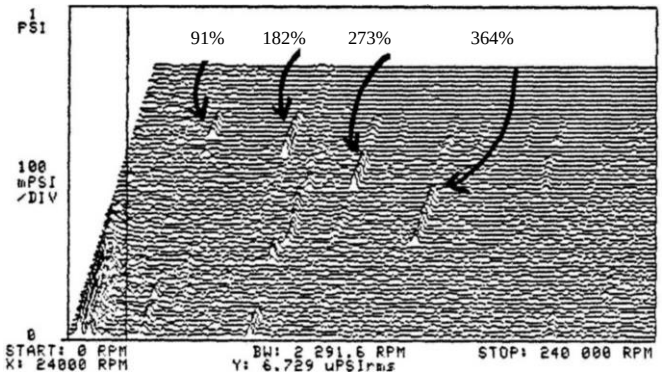

Figure 20. Waterfall plot showing shift in frequency with flow.

Dynamic pressure probes at the exit of one impeller clearly showed that, when the 91% of running vibration appeared, there was a single stall cell rotating at 91% of the rotor speed. This resulting unbalanced pressure force above the impeller caused the rotor response. When the stall mode shifted to two cells, the probes proved that the 182% of running pulsation was actually the result of two cells (180° apart) rotating at 91% of running speed. Because the two pressure disturbances were diametrically opposing one another, the rotor forces were balanced. Similarly, when the 273% of running frequency was apparent, the result of three cells (120° apart) rotating at 91%, the pressure forces on the rotor were again balanced (Figure 21).

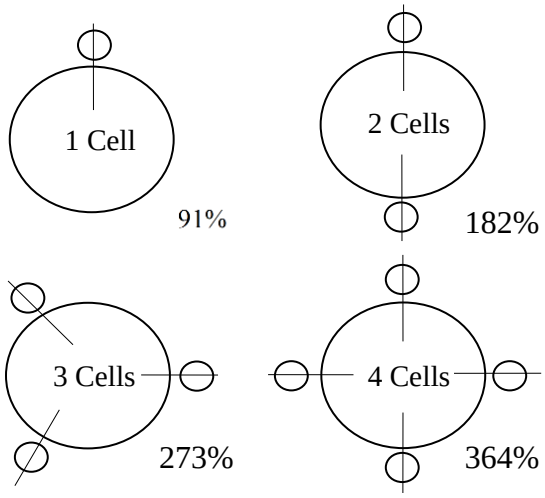

Figure 21. Orientation of stall cells.

The observed behavior of the rotating stall experienced in this compressor does not conform to any of the published characteristics for impeller stall and yet it was obvious that the impellers were creating (or at least amplifying) the phenomenon. In an effort to identify the root cause of the stall, a CFD study was conducted on the impellers. These analyses did show larger than normal amounts of secondary flow at the impeller exit. It was concluded that leading edge incidence [though within prior experience with this impeller] and the aerodynamic loading on the blading were contributing to the high level of secondary flow. The impeller was redesigned to address these two issues and the problem was resolved.

The reason for providing so much detail on this case is that the original stage design adhered to all 1-D criteria existing at that time for stall avoidance and yet a problem occurred. Further, the stall's behavior was very unique and did not conform to any published material regarding the characteristics of rotating stall in centrifugal compressors. In short, this experience provided information on a form of impeller rotating stall not previously encountered. Clearly, more rigorous acceptance criteria were needed to properly assess the potential for centrifugal impeller rotating stall. Such criteria could not be based solely on simple 1-D calculations, though new 1-D guidelines were developed in light of this experience. The more obvious solution which was implemented was to make more effective (and frequent) use of 2-D or 3-D analyses.

Two more crucial observations must be made. First, as noted, the subsynchronous vibration was only evident when the compressor was run at full-load and full-pressure. Had only the class III test been done, the stall would not have been detected until the compressor was installed at the customer's site. Resolution in the field would have been far more difficult and time-consuming. Clearly, there are significant advantages to performing full-load, full-pressure testing prior to shipment of the compressor from the vendor's facilities.

Second, much of the research work done on rotating stall (impeller, diffuser, etc.) has been done using low pressure test vehicles; i.e., single stage test rigs. As was seen in the above example, it may not be possible to quantify the influences of stall or even detect their presence during such low pressure testing. Therefore, it would be more advantageous to conduct rotating stall research using high pressure test vehicles.

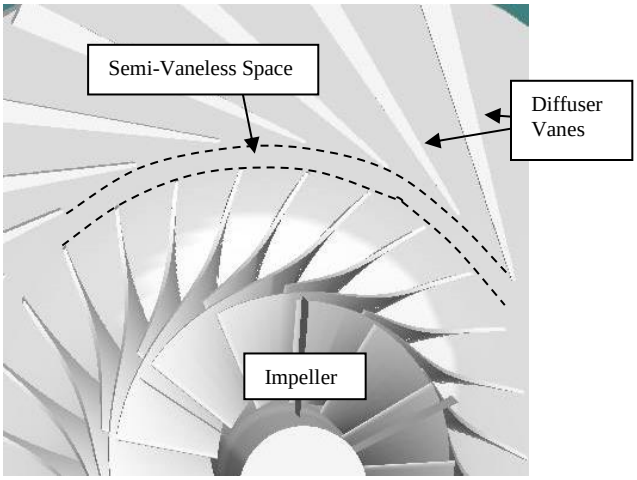

Figure 22. Spacing between impeller and diffuser vanes.

DIFFUSER ROTATING STALL

Though this section is intended to address the entire subject of diffuser rotating stall, the primary focus will be on vaneless diffusers or the vaneless portion of vaned diffusers; i.e., the portion between the impeller and diffuser vanes (the "semi-vaneless space") or between the diffuser vanes and the downstream component (return bend or volute). Some comments on the vaned portion are offered but the majority of the rotating stall problems encountered in vaned diffuser stages arise in the vaneless portion of those diffusers. Recall, problems associated with stationary stall in vaned diffusers were noted previously.

Vaned Diffusers

As noted, stall can occur in the vaned portion of a diffuser. The primary cause is leading edge incidence, though poor passage area distribution or vane design can also contribute. For example, if the passage area at the exit of the diffuser is made too large, leading to excessive diffusion in the vaned passages, the flow will separate from the vanes and large regions of low momentum or reversed flow will form. Whether due to excess incidence or excess diffusion, the result will be flow separation from the vane surfaces or side walls. If the flow separation causes vortex shedding, this shedding might contribute to the formation of rotating diffuser stall in the vaneless space upstream of the diffuser vanes by coalescing into a larger disturbance that propagates at frequencies much lower than those typically associated with vortex shedding. Regardless of whether stationary or rotating, the disturbed flow field can hinder the performance of downstream components, yielding higher losses and a reduction in operating range. The incidence or separation effects can also cause disturbances in the flow field upstream of the diffuser vanes (backflow) or may, in fact, be the consequence of some upstream disturbances; i.e., impeller secondary flows, etc. In fact, it may be possible to initiate rotating stall in the vaned portion of a diffuser if the diffuser follows an impeller which is experiencing rotating stall. Since the stall cells exiting the impeller will be rotational in nature, angular momentum will force the "cells" to rotate through the vaned diffuser. Of course, as the "cells" impact the diffuser vanes, they will be disturbed or possibly eradicated. In fact, some have suggested that low solidity vaned diffusers can be effective in eliminating diffuser rotating stall (*i.e.*, Cellai *et al*, 2003).

However, should the stall cells form and not be eradicated by the diffuser vanes, the resulting non-uniform pressure field can cause significant unbalanced forces on the rotor, especially when the vanes are closely coupled to the impellers (Sorokes and Welch, 1992) (Figure 22). Consideration must be given to the incidence swings that might occur as the end user operates the compressor. If it is clear that one or more of the required operating conditions results in high incidence; i.e., in excess of 10°; there is a high probability that flow separation and the associated stall will occur.

It is difficult to characterize the radial vibration frequencies that arise due to stall in the vaned portion of a diffuser. Unfortunately (or fortunately), there is limited data available in which stall was attributed directly to the vaned diffuser. Some have reported frequencies that are proportional to the number of impeller blades or diffuser vanes; i.e., blade or vane passing. Others (nearly all associated with low solidity vaned diffusers, LSD's – see Figure 23) have cited subsynchronous frequencies in the same range as would be expected for stall in a vaneless diffuser. In the latter case, it has been speculated that the stall actually formed in the vaneless space between the impeller and diffuser due to either: a) highly tangential vaneless space flow angles; or b) high levels of incidence leading to stall cell formation.

Figure 23. Low solidity diffuser vanes (LSDs)

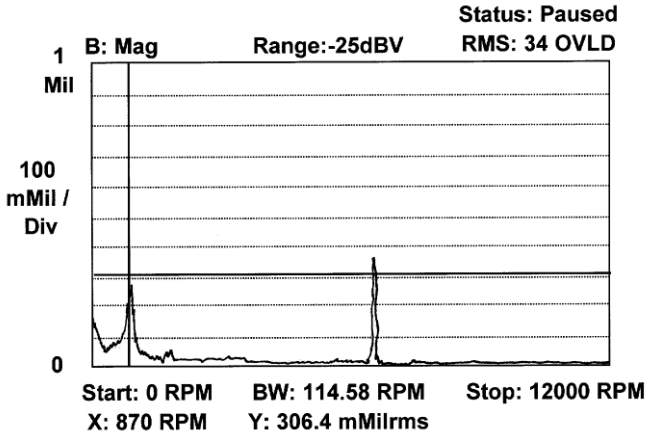

Figure 24. Radial vibration spectrum with LSD's installed.

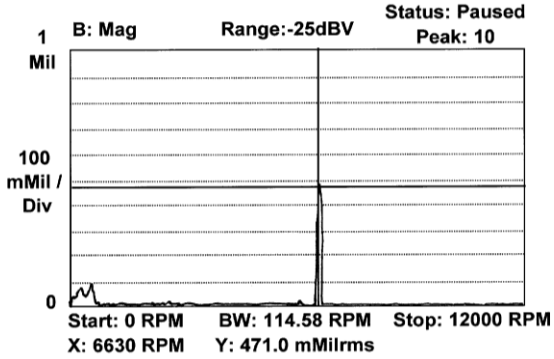

Figure 25. Radial vibration spectrum with LSD's removed.

Examples of Stall Associated with Vaned Diffusers

Despite building and testing a very large number of compressors which employed LSD's and other vaned types (i.e., wedge, airfoil, rib), the OEM has encountered very few cases of subsynchronous vibration or stall which were directly attributable to the diffuser. In the majority of these instances, the situation was rectified by re-staggering the diffuser vanes; i.e., adjusting the vane inlet angles to better match the impeller exit flow conditions. The frequency spectra resulting from the inappropriate setting angles showed both subsynchronous (12% - 25% of running speed) and super-synchronous (blade/vane passing) components.

The OEM had two experiences in the late 1990s in which re-staggering the diffuser vanes did not eliminate the subsynchronous vibrations. In these situations, the compressors were tested with one or more vaned diffuser arrangements and, finally, with vaneless diffusers. When the vanes were removed, the subsynchronous vibration was still apparent but at reduced amplitude as compared to the test with the vanes installed. Consider the frequency spectra given in Figures 24 and 25. The spectra in Figure 24 were taken during a near surge excursion with the LSD's installed. The spectra shown in Figure 25 were taken at the same flow condition after the LSD's were removed. Clearly, the amplitude was reduced when the LSD vanes were not present, yet a response was still evident. In short, the LSD vanes were serving as "reflectors" which amplified the effect of stall cells thought to be forming in the semi-

vaneless space immediately outside the impeller exit. With the vanes in place, these stall cells or pressure disturbances were being reflected between the impeller and the diffuser vanes, causing unbalanced radial forces on the rotor. Without the vanes to serve as "reflectors", the blade - vane interactions was eliminated and the rotor vibrations reduced.

Calculations of the flow angles in the semi-vaneless space showed that, while incidence on the LSD vanes was minimal (i.e., approximately -2°), the flow angles exceeded the critical angle for vaneless diffuser stall (more detail in following sections). The calculations supported the contention that the stall was occurring upstream of the LSD vanes.

The diffuser passages were contracted to move the flow angle out of the stall regime and new LSD vanes were designed to match the more radial flow angles. Upon retesting the compressor, no subsynchronous vibrations were encountered at any flow condition within the required operating range.

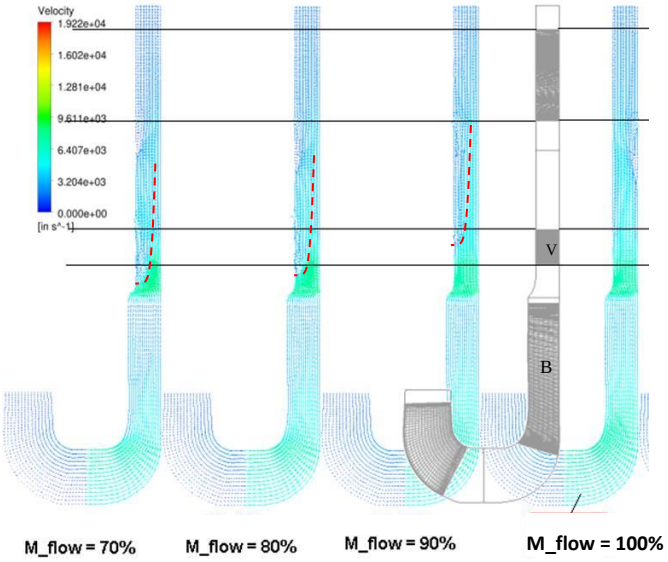

Figure 26 – CFD analyses related to stall associated with low solidity vaned diffusers

More recently, computational fluid dynamics has been helpful in investigating stall issues associated with vaned diffuser applications. As one example, the OEM experienced a stall issue on a high pressure Legacy compressor that contained low solidity vaned diffusers. To investigate the situation, CFD analyses were conducted on the last stage impeller of the compressor at various conditions covering the flow range in which the stall appeared. The CFD did indicate that a low momentum zone formed along the shroud side of the diffuser. Red dashed lines have been added to the results shown in Figure 26 to indicate the location of the low momentum zone. The geometry is also included in Figure 26 to indicate the location of the impeller blades (labeled "B") and diffuser vanes (labeled "V". The lowest horizontal line in the figure overlays the diffuser vane leading edge radius on the CFD results.

The CFD analyses indicate that the low momentum zone extended upstream of the diffuser vane leading edge at or near 80% of the design flow rate. This agreed very well with where the stall occurred on the test stand. The agreement led to the conclusion that the stall formed when the low momentum zone was in the semi-vaneless space between the impeller and the diffuser vanes. Alternate diffuser geometries were developed that kept the low momentum zone out of the semi-vaneless space. This configuration was then applied to the compressor and the unit experienced no subsynchronous vibrations on test. [Note: Due to the proprietary nature of these modifications, the final results cannot be published.]

In summation, vaned diffusers can be the source of stall-related phenomena; the result of high levels of positive or negative incidence. They can also accentuate vibration resulting from stall cells rotating in the semi-vaneless area between the impeller and vaned diffuser. Conversely, experience has also shown that installation of vaned diffusers can also eliminate and/or delay the onset of rotating stall provided the vanes are placed in the region where reverse or stagnated flow begins to form. The designer must be aware of these critical considerations and insure that vane incidence and the flow angles in the semi-vaneless space are within acceptable limits and that the vanes are placed in the most desirable locations.

Vaneless Diffusers

Some of the earliest research into vaneless diffuser rotating stall was conducted by Dr. Willem Jansen (1964). Jansen was investigating stall in vaneless diffusers caused by localized non-uniformities in the radial gas velocity. He determined that these non-

uniformities lead to pressure disturbances or "stall cells" that rotate circumferentially around the compressor, subjecting the rotor to unbalanced pressure forces. Jansen's work showed that the onset of diffuser rotating stall was most strongly influenced by the diffuser flow angle. Once the diffuser angle exceeded some critical angle, rotating stall occurred. Depending on the flow conditions and the details of the diffuser geometry, single or multiple stall cells (i.e., 2, 3, 4, etc.) can form. The rotor vibration characteristics will be a function of this number of cells and their rotational speed relative to the compressor operating speed.

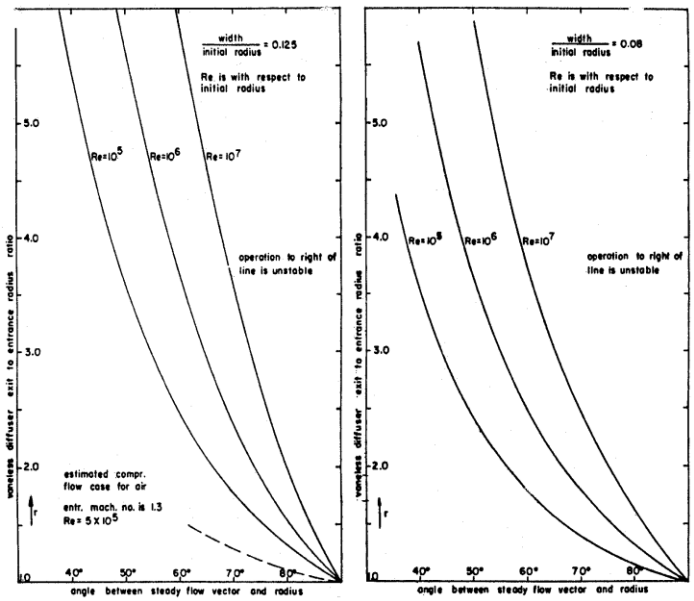

Figure 27. Jansen criteria for rotating stall avoidance in vaneless diffusers.

The flow angle in a diffuser is a function of operating conditions as well as the details of the diffuser geometry. Jansen's studies showed that the critical angle for the onset of rotating stall is also a function of the diffuser geometry and the gas Reynolds Number. To aid designers in their efforts to avoid rotating stall, Jansen developed a series of guidelines or correlations which showed how the critical angle would change for various diffuser geometries and Reynolds numbers (Figure 27).

Subsequent research into rotating stall sought to further refine these guidelines or correlations. Among these were the efforts of Y. Senoo (1977, 1978a, 1978b), A. Abdelhamid (1980, 1985), A. Abdelhamid et al (1979, 1980) and Frigne/Van den Braembussche (1984). Y. Senoo published several papers in the late 1970's that included criteria that became widely accepted by the compressor industry. Prof. Senoo had sought to identify other parameters that influenced the critical angle for diffuser stall. He found that Mach number, Reynolds number, radius ratio, contraction ratio (ratio of diffuser width to impeller tip width), and, most notably, velocity distortion at the diffuser inlet all played an important role in determining the critical angle. This latter parameter is quite important because it suggests that the more disturbed the impeller exit flow profile, the greater the likelihood that the downstream diffuser will stall.

Kobayashi, Nishida et al (1988, 1990) expanded on the Senoo work, investigating the effects of diffuser inlet profile on Senoo's criteria. They found that the rate of diffuser pinch and the general shape of that pinch (i.e., the diffuser hub and shroud entrance geometry) can have significant influence on the accuracy of the Senoo methods. Interestingly, their work showed that rotating stall could occur at higher flow (i.e., more radial flow angles) if there is excess area above the impeller exit. This situation seems to be more critical in lower flow coefficient stages. Sorokes (1994) supported this contention in his work based on CFD (computational fluid dynamic) analyses of various diffuser entrance geometries.

Despite all of the published literature and ongoing research (notably the Concepts ETI rotating stall consortium), like impeller rotating stall, there remains no definitive set of criteria for rotating stall avoidance in vaneless diffusers. However, experience has shown that conservative application of the Senoo criteria can yield a very high rate of success in avoiding diffuser stall. For example, insuring that the diffuser flow angles do not come within 3 - 5° of the critical angle based on the Senoo criteria typically will insure rotating stall avoidance in most cases (Figure 28). Of course, it is crucial that the flow angles be assessed over the entire required operating range for the compressor; i.e., from design flow back to the surge control line.

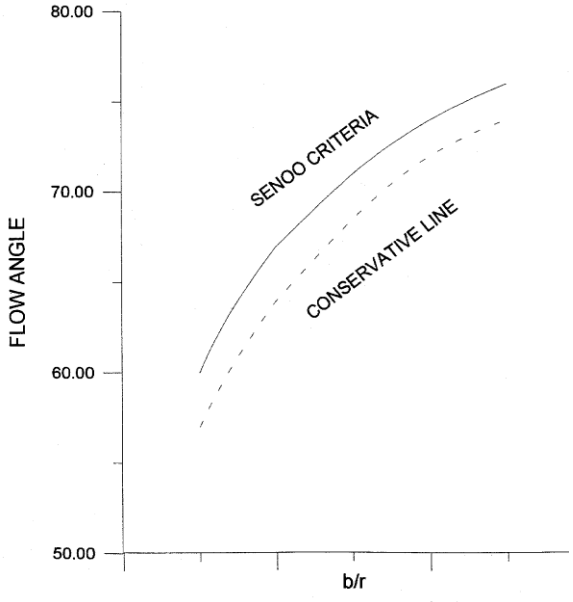

Figure 28. Senoo criteria for stall avoidance showing conservative line.

Vaneless Diffuser Rotating Stall Characteristics

Compressors experiencing subsynchronous vibration due to diffuser rotating stall exhibit some or all of the following characteristics:

- The subsynchronous radial vibration frequency is in a range of 6% to 33% of running speed.
- The vibration frequency is sensitive to flow rate and, after onset, will typically increase as the flow rate is reduced.
- The vibration frequency tracks with speed as long as Q/N is held fairly constant.
- There is a hysteresis zone associated with the onset flow rate. That is, when reducing flow, the phenomenon will appear at some flow rate. However, the vibration does not disappear simply by moving back above that flow rate. Instead, operators have to increase flow significantly beyond that rate to "wash out" the stall cells.
- There may be sudden jumps in frequency as the stall progresses from one to two to three cells, etc.
- If dynamic pressure probes are available, their output shows a response in the 6% - 33% range. They also show a frequency spectrum consisting of numerous harmonics of some basic frequency. The spectrum appears as would a "clipped square wave."

Examples of Stall Associated with Vaneless Diffusers (or vaneless passages)

Vaneless Diffuser

Rather than cite specific compressors which experienced diffuser rotating stall, this section provides an overview of the two most common reasons that the phenomenon arises in industrial turbomachinery. This section also describes how a stall can form in other vaneless portions of the flow passage and addresses two examples of such.

Vaneless diffuser rotating stall can occur if designers do not account for assembly tolerances within a compressor. Another common reason is improper calculation of the upstream impeller exit flow angle causing an inaccuracy in specification of the diffuser width necessary for stall avoidance. That is, the calculated impeller exit flow angle is more radial than in actuality, resulting in insufficient diffuser pinch and a diffuser flow angle which is too tangential.

Returning to the subject of assembly tolerances, it is common practice to allow machining or assembly tolerances on the parts (return channels, guide vanes, inlets, discharge volutes) that stack together to form the compressor flow path. When the unit is operated, any gaps between components (created by the machining or assembly tolerances) will be closed as the pressure builds on the walls of the various flow passages. All walls will deflect away from the point of highest pressure within the machine. In a compressor, the highest static pressure occurs in the last stage diffuser. Therefore, the walls of that diffuser will move apart as any machining or assembly gaps present in the remaining components are closed. Failure to account for the growth of this diffuser width can have significant consequences.

Most past occurrences of diffuser rotating stall encountered by the OEM were caused by the deflections described above. At operating pressures, walls deflected, the last stage diffuser width increased, the diffuser flow angle increased (became more tangential), and rotating stall developed. The machines exhibited low frequency subsynchronous radial vibrations in the range of 6% to 33% of the running speed, though the majority fell in a 6% to 18% range. The excess vibration typically arose as operators throttled the compressor toward the surge control line and, once present, would remain until the compressor was moved to much higher flow rates. Again, since the vibrations come and go at different flow rates, the phenomenon is said to have a hysteresis zone.

In all but limited cases, the stall was eliminated by reducing the diffuser widths such that, at pressure, the deflections would not result in flow angles which reached the critical level necessary to instigate rotating stall (see Figure 29 for typically corrective measure). It is clear that manufacturing tolerances and material deflection under pressure must be accounted for to insure stall avoidance.

In a small number of cases, rotating stall was eliminated by installing low solidity vaned diffusers (LSD's). Such diffusers delay the onset of rotating stall by influencing the growth of secondary flows and boundary layers which promote stall inception. LSD's are a more attractive option when dealing with low flow coefficient stages. In such cases, the amount of vaneless diffuser pinch necessary to insure proper flow angles often would produce unacceptable efficiency loss. The LSD eliminates this concern by allowing stable flow to be maintained with wider passages. Of course, in designing the vaned diffuser, one must avoid creating different forms of stall caused by vane incidence effects. (See Vaned Diffusers above.)

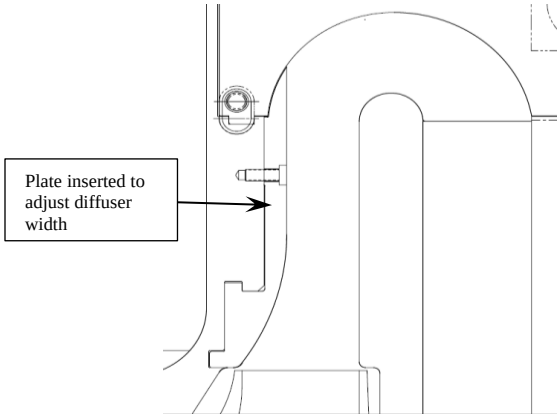

Figure 29. Typical Diffuser Correction.

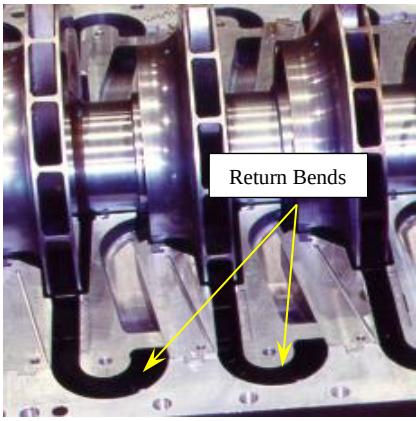

Figure 30. Return bends (vaneless space).

Return Bend

Another form of vaneless space rotating stall can occur in the return bend (the 180° bend between the diffuser exit and return channel entrance -- Figure 30) as reported by Sorokes et al (1994). Though not typically considered part of the diffuser, the return bend does constitute a vaneless space and, therefore, is a potential location for stall inception. In fact, since area typically increases through the 180° bend, there is a greater tendency for secondary flows to arise and form rotating stall cells. Little or nothing can be found in the open literature regarding rotating stall in this element. However, there has been strong evidence for such in at least two instances.

In both cases, the return bend designs fell within previous experience, implying that there was little reason to suspect any potential for stall. In addition, the diffuser widths upstream of the bends were very conservatively sized to avoid rotating stall. Similarly, the impellers adhered to all known criteria for stall avoidance. Therefore, it was very surprising when subsynchronous radial vibrations arose. The subsynchronous frequency was in the range characteristic of vaneless diffuser stall. The frequency spectra and wave forms also bore a strong resemblance to those generated by diffuser rotating stall.

A review of the flow angles in the various stage components identified rather high tangential angles in the return bend passages. While the diffuser flow angles were well below the critical level for rotating stall, the flow angles in the return bend were not. In short, despite having no prior experience with stall in a return bend, the data indicated that the stall was occurring in the bends and not in the diffuser passage.

In the first of the two cases, the stall was eliminated by reducing the return bend passage widths in all stages. In this instance, the diameter to the entrance of the bends was not changed; implying no change in the tangential velocity component. The decreased passage width effectively increased the meridional velocity and, therefore, reduced the gas flow angle.

In the second compressor, in addition to a reduction in cross-sectional passage width, the radius to the entrance of the return bend was decreased. The change in radius and passage area caused both the gas tangential and meridional velocity to increase. However, the meridional velocity, being a function of both the radius and the passage width, increased by a larger percentage than did the tangential velocity. The result was a decrease in gas flow angle of approximately 5° at any given flow condition. As with the first case, the stall and associated subsynchronous radial vibration were eliminated from this compressor.

In these two cases, the machines exhibited characteristics that could have been interpreted as diffuser rotating stall, yet the stall was not caused by the diffusers. Without careful review of all of the geometry and available data, analysts may target the wrong components for corrective measures.

Because of these experiences, it is now common practice to assess the flow angles through return bends using much the same criteria as applied for vaneless diffusers. Logic suggests that if the flow angles are too tangential for a vaneless diffuser, they should likewise be too tangential for a vaneless return bend.

INTERACTION "STALL"

Non-uniform pressure fields can be formed through the interaction of components or the interaction of the pressure fields created by adjoining components. It is not clear that these phenomena should be characterized as rotating stall. Still, they do cause a rotating non-uniform pressure field which imposes unbalanced forces on the rotor and their influence on said rotor mimic those of true rotating stall. Therefore, it is appropriate to associate these phenomena with rotating stall.

Impeller - Diffuser Interaction

The most common form of impeller - diffuser interaction occurs when one wall of a diffuser abruptly overlaps the impeller exit gas passage, causing an obstruction in the flow path. The flow impinging on the obstruction causes pressure disturbances which can influence the rotor. Such a situation can be avoided by proper flaring of the diffuser entrance, thereby insuring that detrimental overlap cannot occur. Of course, one must be cognizant of the axial movement of the rotor during operation at various flow conditions.

This form of interaction stall can occur at either end of the performance map (i.e., toward overload or toward surge). At high flow rates, the impeller exit flow angle is more radial and there is more kinetic energy in the gas stream. Consequently, the energy involved in the interaction is higher, resulting in greater forces acting on the rotor. Further, as one reduces flow and the angle becomes more tangential, it is easier for the flow to "slip around" the obstruction without causing feedback to the rotor. However, the obstruction can also accelerate the onset of stall at tangential flow angles by promoting separation from the diffuser walls.

There are no generally accepted characteristics for impeller - diffuser interaction stall. However, the following loose criteria are offered:

- The frequency range is approximately 20% - 50%(?) of running speed
- There is no hysteresis zone
- The frequency is sensitive to flow rate but may not appear sensitive to speed
- The subsynchronous vibration amplitude will be sensitive to rotor running position
- This phenomenon can occur at high rates; i.e., toward the overload end of the performance map.

As a final comment on this form, it might appear immediately after an overhaul or rotor change-out if care is not taken to properly align the impellers to the diffuser openings.

Diffuser Volute Interaction

A second form of interaction stall which has gained interest in the turbomachinery world is interaction between the diffuser and the discharge volute. Some hold that this form should be lumped under vaneless diffuser stall since the phenomenon is caused by interaction of diffuser stall cells (or the rotating non-uniform static pressure field) with the volute tongue (or tongues). As with all other forms of stall, the result is unbalanced pressure forces on the rotor, leading to rotor vibrations.

What makes this form of interaction stall so troublesome is that it can easily be misinterpreted as impeller stall because of the frequencies involved. Recall that diffuser stall is characterized by frequencies in the 6% to 33% of running speed range. Suppose now that there are three diffuser stall cells (or three lobes in the pressure field) rotating at 20% of running speed. These "cells" will each interact with the volute tongue in one revolution of the pressure field. Since sensitive to the interaction of each "cell" with the tongue, the rotor response will be at three (the number of "cells") times the rotational frequency of the pressure field (20% of running) or *60%* of running speed. The analyst might be misled into believing the problem is impeller stall. However, since rooted in diffuser rotating stall, the phenomenon will exhibit a hysteresis zone, thus distinguishing it from impeller stall.

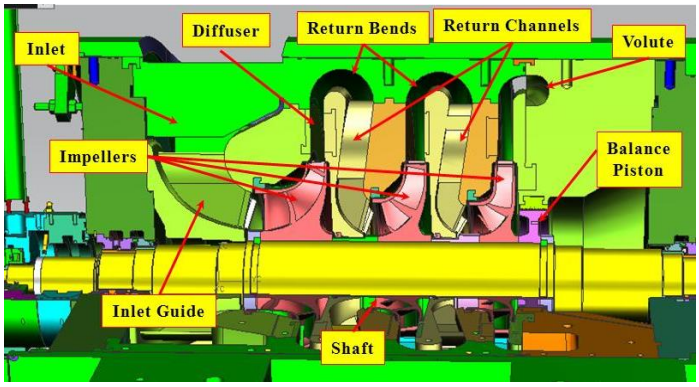

Figure 31. Compressor cross-section

Other Components

Since rotating stall is the consequence of any non-uniform pressure field rotating within the compressor, anything which contributes to the formation of such non-uniform fields can cause some form of rotating stall. Possible contributors include:

- flow in impeller recess areas (the cavities which surround the rotating impellers),
- eccentric rotors (area varies circumferentially causing flow velocities to vary resulting in non-uniform static pressure)
- non-uniform pressure fields caused by inlets, volutes, sidestreams, etc.

In short, any flow carrying passage within a compressor (see Figure 31)

It would be nearly impossible to characterize all of the frequencies, wave forms, etc. that could result from the anomalies listed above. Suffice to say, if the more common phenomena (impeller and diffuser stall) can be effectively eliminated from consideration, one must look elsewhere for the source of the forces causing subsynchronous vibration.

NUMERICAL METHODS

Since the original release of this paper in 2000 and as noted in the vaned diffuser section, many have investigated the use of unsteady CFD analyses to predict the occurrence of rotating stall with varying degrees of success [*i.e.*, Gourdain *et al*, 2006; Izmaylov et al, 2012; Vezier *et al*, 2013, and DeMore *et al*, 2014]. Many factors influence the ability of the numerical methods to predict the stall phenomena. The factors include but are not limited to:

- the turbulence models used by the code
- the grid density
- the details captured by the computational domain; i.e., are all secondary flow passages or flow path discontinuities included in the model?

- the boundary conditions imposed
- whether or not periodic boundaries are used: i.e., a sector model v. full 360° model
- the grid interfaces applied; i.e., circumferential averaged, frozen rotor, etc.

All of the above can artificially lead to the types of pressure and/or velocity disturbances that might be interpreted as rotating stall. For example, if a numerical simulation is run on a compressor stage using a 90° "pie-slice" with periodic boundary conditions and the results suggest there are two pressure or velocity disturbances in the resulting flow field, one must take steps to ensure the disturbances are truly the result of a flow field issue and not the result of the periodic boundaries.

One should also remember that virtually all CFD studies are conducted using design models / dimensions. Small variations due to manufacturing and/or assembly tolerances are not reflected in the models used. Therefore, it is possible that the numerical simulations will not include the geometric variations that could lead to the formation of the stall phenomena; i.e., subtle variations in the width of a vaneless diffuser that could lead to non-uniform circumferential pressure distributions.

Another consideration is the amount of time it takes to run unsteady CFD analyses. Despite the tremendous gains in computational speed, such analyses still take days to converge, making use of such codes in the day-to-day design process impractical. However, as computer speeds continue to increase and the CFD codes evolve, such numerical simulations could become instrumental in rotating stall avoidance.

VIBRATION SIGNALS

Each of the various types of vibration signals one might see are discussed below. It is assumed that an FFT signal analyzer is available, to put the signal in the frequency domain. Although the best way to visualize and describe these signals with such an analyzer is to view them in real time, a reasonable alternative is to view a series of snapshots of the signals at varying times. This is preferable to the often used "peak hold" mode of the typical analyzer, since it doesn't hide the variation in amplitudes and frequencies that are occurring at levels underneath the maximum amplitudes.

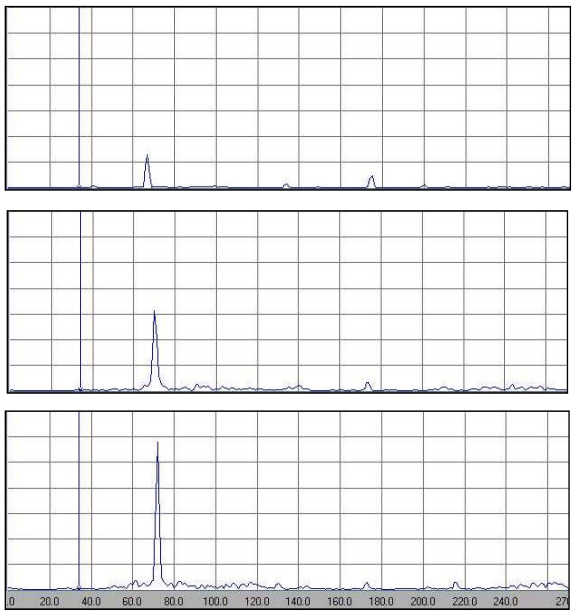

Figure 32. Spectra from vibration probe during rotor instability.

Free Vibration

As noted earlier, "free" vibration is typically seen only as what is commonly called "rotor instability". A typical example is shown in Figure 32. The frequency of interest (66-72 Hz in this case) is the first natural frequency of the rotor. The signal appears at a relatively low amplitude initially (top spectrum in Figure 32), but increases in amplitude as an operating parameter such as discharge pressure is increased, until it increases dramatically on its own, without changes in operating conditions. Eventually, the vibrations reach trip level (bottom spectrum in Figure 32) and the unit shuts down.

In this particular case, although no speed change of consequence occurred to show the lack of relationship between the rotating speed and the natural frequency, the change in the natural frequency as it begins to increase and then dominate the vibration of the rotor, demonstrates its independence relative to the RPM. Also note the relative absence of components of the vibration at other frequencies. All we can see of consequence is the natural frequency and the running speed of the machine, which is the peak at 173-175 Hz.

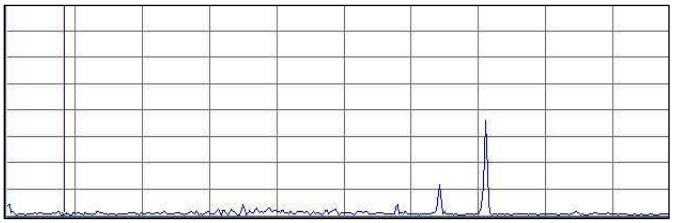

(a) 142 Hz running speed

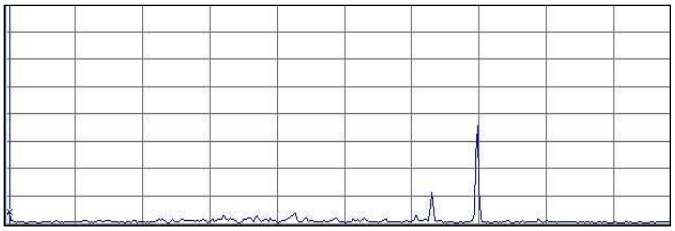

(b) 140 Hz running speed

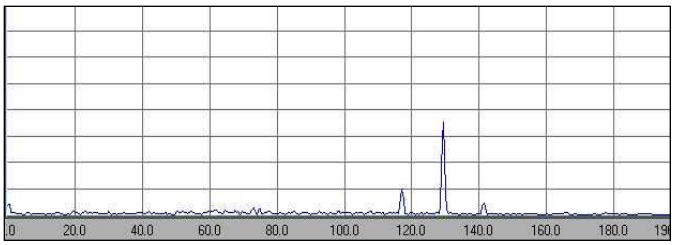

(c) 130 Hz running speed

Figure 33. Variation in subsynchronous vibration frequency with running speed.

Forced Vibration

Harmonic Force

As discussed earlier, an impeller stall is a good example of a relatively clean single frequency subsynchronous harmonic force. In Figure 33 we see a signal at 117-128 Hz due to such a stall. The unit is running at 130-142 Hz, as indicated by the larger synchronous vibration signal. Note that the subsynchronous signal stays at a constant 89-90% of the running speed, changing frequency with changes in speed from Figure 33a at 142 HZ running speed, to Figure 33b at 140 Hz, and Figure 33c at 130 Hz running speed. Other characteristics of note are the relatively steady amplitude at the stall frequency, and the lack of other significant components of the vibration.

The freedom of harmonics in this vibration signal is illustrated in Figure 34. The same unit is running at 150 Hz in this instance, with the stall frequency at 134 Hz. The frequency scale is set at three times the running speed, making it evident that no multiples of the stall frequency are present, at least at noticeable amplitude levels, in the vibration signal. Other characteristics specific to impeller stall, such as the lack of hysteresis when changing flow, and the ability to make the signal disappear by flow reductions (changing numbers of stall cells) are difficult to present without live presentations of the data.

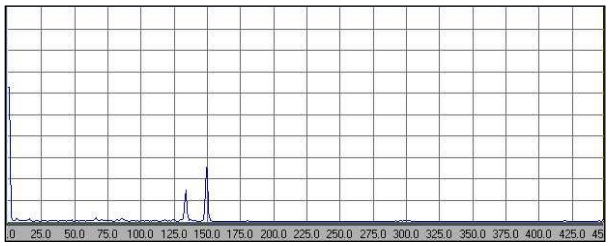

Figure 34. Radial vibration spectrum during impeller stall.

Periodic Force

Impeller and diffuser stall are both good examples of periodic forces. As noted previously, the pressure disturbances caused during stall rotate at speeds lower than the rotor, resulting in subsynchronous radial vibrations. Typical frequency spectra for impeller and diffuser stall are given in figures 35 and 36, respectively. In each figure, the top trace (a) is the vibration probe signal immediately prior to onset of the stall. The second trace (b), also taken just prior to the onset of stall, is from a dynamic pressure transducer in the diffuser immediately outside the impeller for the impeller stall case or at the exit of the diffuser in the diffuser stall case. The third trace (c) is from the vibration probe after onset of stall and the fourth trace (d) is the dynamic pressure transducer output after onset.

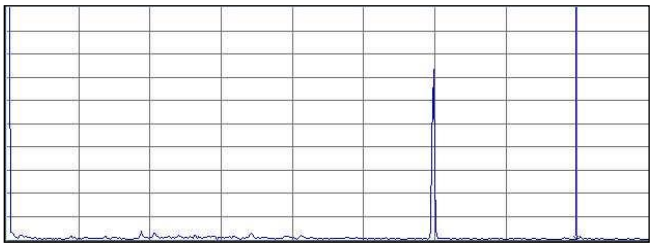

(a) vibration spectrum prior to onset

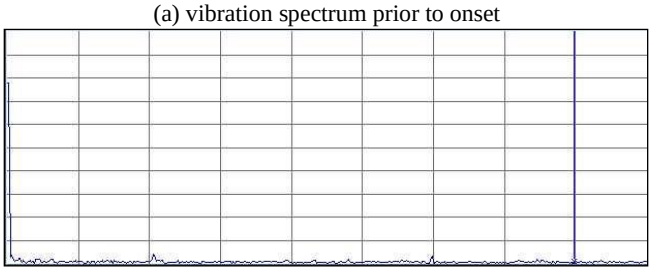

(b) dynamic pressure spectrum prior to onset

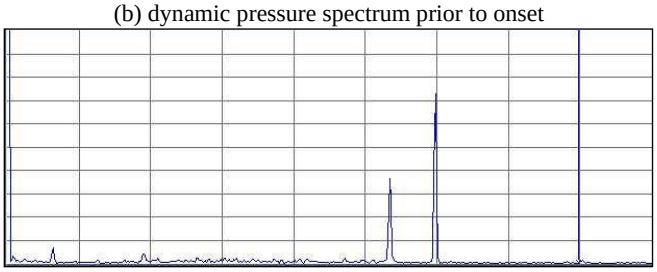

(c) vibration spectrum after onset of impeller stall

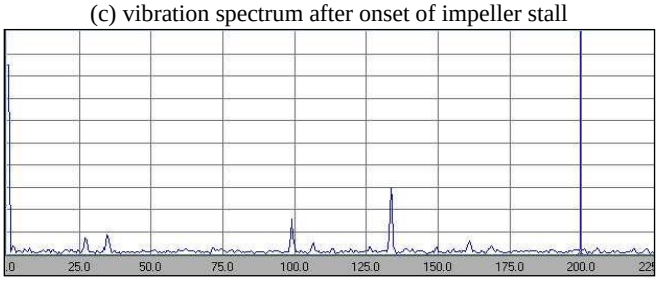

(d) dynamic pressure spectrum after onset of impeller stall

Figure 35. Vibration and dynamic pressure spectra before and after onset of impeller rotating stall.

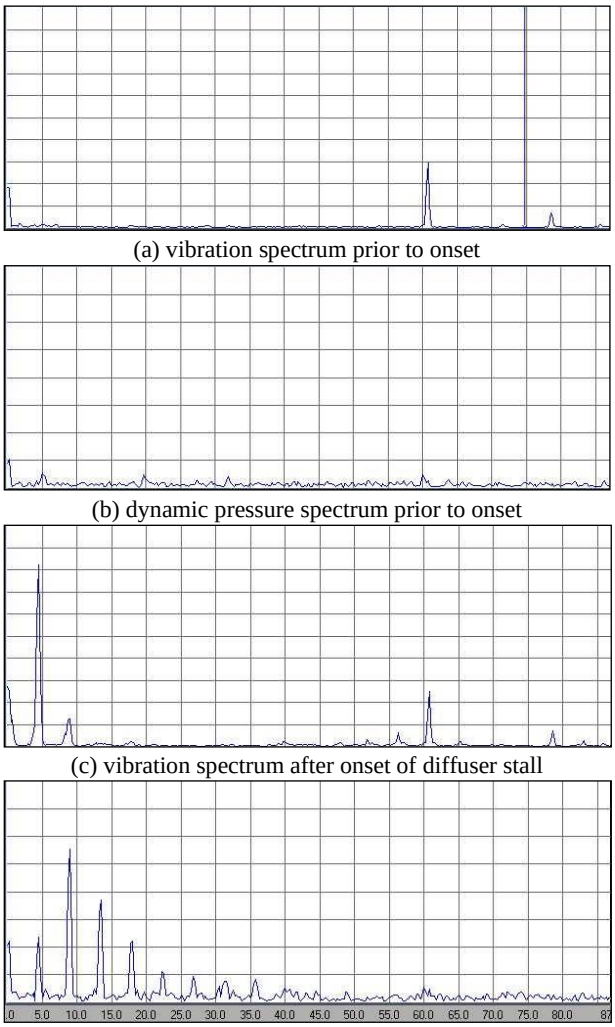

(a) vibration spectrum prior to onset

(b) dynamic pressure spectrum prior to onset

(c) vibration spectrum after onset of diffuser stall

(d) dynamic pressure spectrum after onset of diffuser stall

Figure 36. Vibration and dynamic pressure spectra before and after onset of diffuser rotating stall.

Clearly, in the case of impeller stall (Figure 35), forced vibration is only occurring due to the stall at 133 Hz. Also note that the 1X frequency (149 Hz) does not appear in the dynamic pressure probe output.

Note that there are multiple harmonics (4.5 Hz, 9.0 Hz, 13.5 Hz, etc.) in the dynamic pressure spectra in Figure 36(d). In this case, the probe was not sensing many cells moving at different speeds. Rather, the multiple peaks represent the FFT's rendition of the typical "clipped square wave" appearance of a diffuser stall wave form, which leads to multiples (harmonics) of the base frequency (4.5 Hz).

Also note that although the pressure signal in Figure 36(d) indicates multiple frequencies present, on the vibration response in Figure 36(c) only the primary and first multiple are evident, at the same frequencies as in the pressure signal. This vibration response is larger at the lower frequencies due to high damping in the system, with relatively low stiffness. Such a result is evident from solutions of simple systems, as shown in Equation 11 above. As indicated, when damping is a significant factor in the response equation, amplitude response for the same force will increase as the frequency is reduced. The high damping values that minimize dangerous vibration response at higher frequencies allow greater response at the low frequencies of this example. In fact, the highest response is at the lowest frequency, while the forcing function is greater at a higher frequency.

In the aero section introduction, emphasis was placed on the difference between surge and stall. To illustrate the difference, consider Figure 37. The trace in Figure 35(a) is from a dynamic pressure transducer in a diffuser passage when said diffuser is in a rotating stall mode. The trace in Figure 35(b) was taken while the same machine was in true surge. Note the extremely low frequencies associated with the surge (approx. 1 Hz).

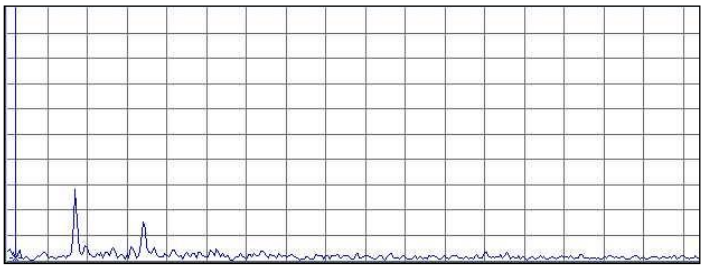

(a) diffuser stall

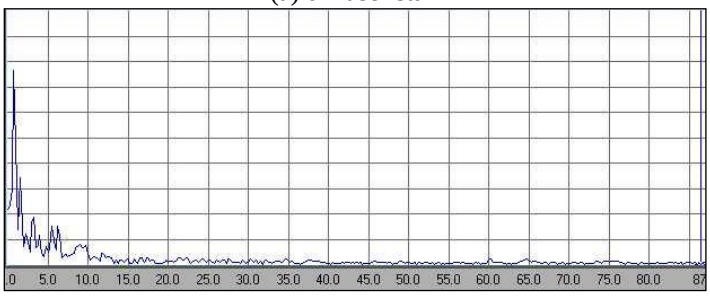

(b) surge

Figure 37. Dynamic pressure spectra - stall versus surge.

The associated raw wave forms for the stall and surge are given in Figure 38. Frequency spectra for the vibration probes under the same conditions (stall and surge) are shown in Figure 39. The distinctions between the two conditions are fairly obvious. Note that surge results in a broad impulse excitation of the rotor that may or may not excite the first natural frequency, depending on the amount of damping in the system, whereas the response to stall is primarily at the stall propagation frequency.

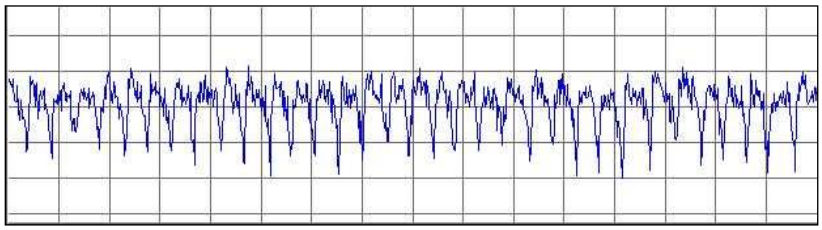

(a) diffuser stall

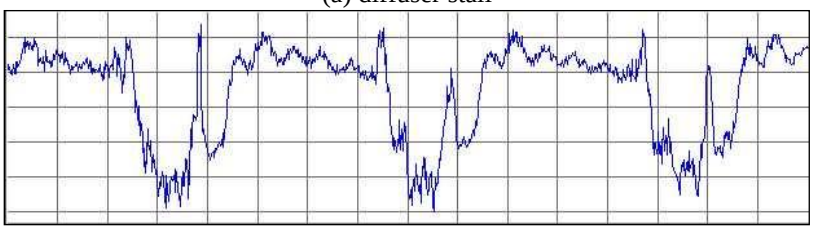

(b) surge

Figure 38. Dynamic pressure wave forms - stall versus surge.

Of course, one must be very careful when attempting to identify the cause of low order subsynchronous vibrations. Other forces acting on the rotor can reflect frequency spectra and/or wave forms like those of the various aerodynamic phenomena. For example, the frequency spectra shown in Figure 40 might be mistaken for diffuser stall. The spike at 63 Hz is the 1X response while the spike or spikes at lower frequencies (5 Hz in Figure 40a; 4.5 Hz and 6.75 Hz in Figure 40b) are the subsynchronous response. Clearly, the subsynchronous frequencies are in the classic range for diffuser stall. However, the shift in the subsynchronous peak occurs at constant flow conditions. In fact, the subsynchronous vibration in this case is caused by a "rattling" seal ring and not by any aerodynamic phenomena. Oil seal rings designed for high pressures may not “seat” properly on the end face at lower pressure test conditions, allowing oil to flow around the seal ring, not just under it. This causes the rattle, which is easily uncovered by adjustments in seal oil pressure. Onset is usually sudden, but as oil pressure is increased, the vibration amplitude will decrease, and the frequency will increase.

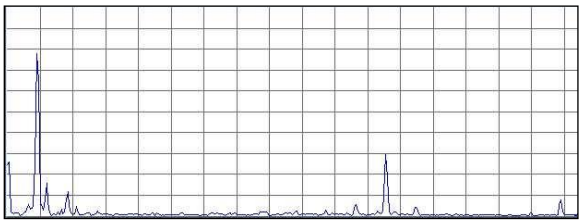

(a) diffuser stall

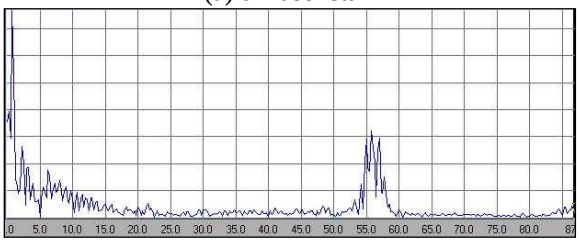

(b) surge

Figure 39. Vibration spectra - stall versus surge.

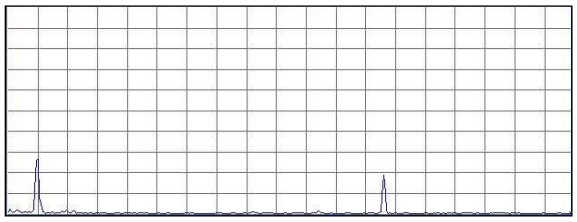

(a) lower seal oil pressure

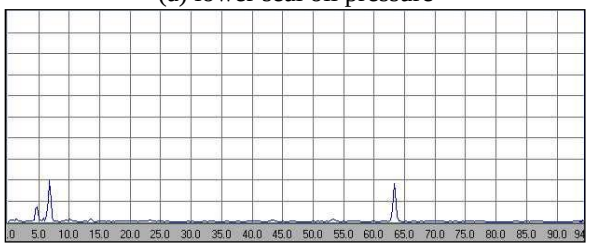

(b) higher seal oil pressure

Figure 40. Vibration spectra - "rattling" seal ring.

Arbitrary Aerodynamic forces

Due to its transient nature, vibration caused by arbitrary forces is very difficult to capture on a sheet of paper. It may be most useful to compare a typically used “peak hold” spectrum with other both specific and random spectrums for the same signal. The peak hold spectrum shown in figure 41 is from 100 seconds of data with a rotor undergoing such forces. It clearly indicates a peak response to these forces just below 25 Hz, at the natural frequency of the unit, with the other major amplitudes at the running speed and at very low frequencies where the high system damping results in high response levels (see earlier comments). Though all levels shown were within specification requirements, the peak at the first natural frequency could be a cause of concern if we just use this plot for evaluation. More investigation is needed to determine the true nature of the vibration.

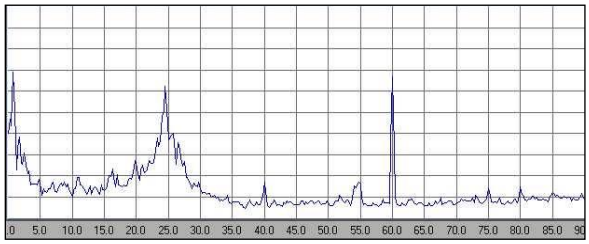

Figure 41. Peak hold vibration spectrum - arbitraryaerodynamic forces.

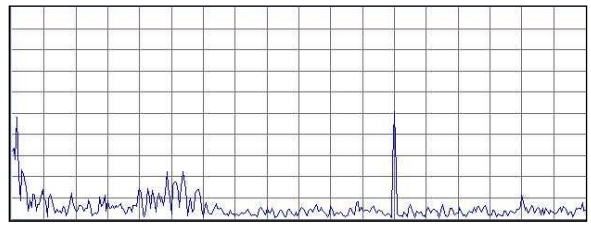

(a) 2 seconds before

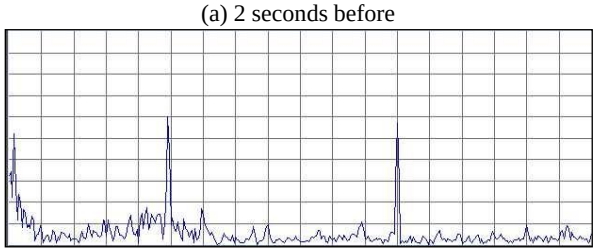

(b) Peak amplitude

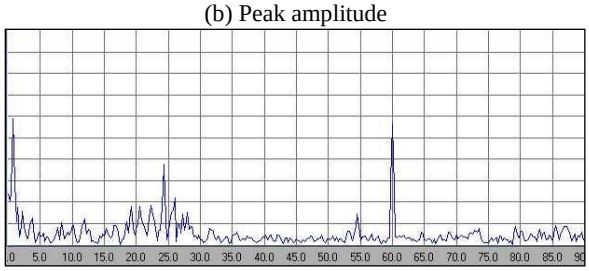

(c) 2 seconds after

Figure 42. Vibration spectra - arbitrary aerodynamic forces.

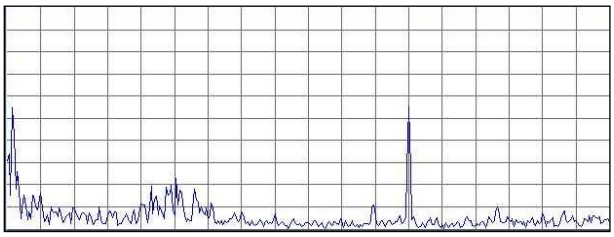

(a) 10 seconds after peak amplitude

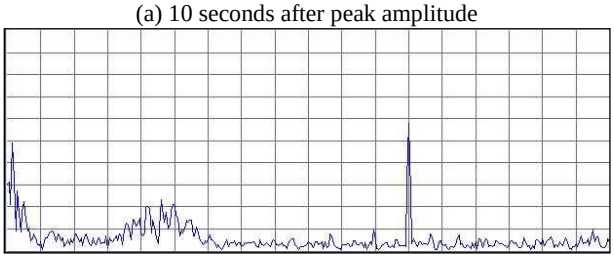

(b) 30 seconds after peak amplitude

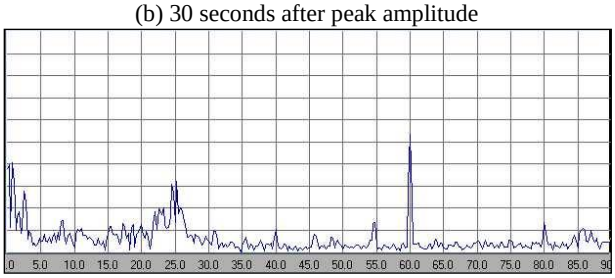

(c) 60 seconds after peak amplitude

Figure 43. Vibration spectra - arbitrary aerodynamic forces.

Figure 42 indicates the vibration spectrum at the time of the highest amplitude at the first natural frequency, as well as the spectrum 2 seconds before and 2 seconds after. Figure 43 indicates the spectrum at 10, 30 and 60 seconds after the peak signal. This data shows

the transient nature, varying amplitude, and varying frequencies typical of response to arbitrary forces. If viewed in real time, such a spectrum would appear to be “dancing” or “rumbling", with amplitude peaks highest in the area of the rotor first natural frequency (approximately 40% of running speed). No "fixed spikes “ exist at any frequency, and the various peaks form and disappear in time, shifting in both amplitude and frequency with no apparent correlation to any operating parameters (i.e., flow rate, speeds, gas conditions, etc.). This is clear evidence of a forced vibration, with the rotor acting in response to external forces within the gas path.

CONCLUSIONS

The forces acting within centrifugal compressors can cause a variety of responses in the rotor system. A general discussion of compressor rotor dynamic behavior was presented including discussions on free and forced vibrations. Distinctions were made between significant subsynchronous vibration characteristics, such as rotor instability, and aerodynamically forced vibration of various types. Ways to distinguish between these various causes using vibration data were also provided.

The various aerodynamic phenomena which contribute to increased radial vibrations were discussed including impeller stall, diffuser stall, and interaction "stall". A general description of the flow physics was provided as were the commonly held identification criteria for each. Finally, various frequency spectra and wave form plots were offered to illustrate how the various phenomena may appear in vibration or pressure pulsation data; i.e., on a spectrum analyzer or oscilloscope.

No single paper can adequately address the entire subject of aerodynamic excitation of rotor systems. Still, it is hoped this document provides the reader with a good general overview of a very complex subject.

ACKNOWLEDGEMENTS

The authors acknowledge the following individuals for their help in generating the figures and other presentation material used in this paper: Chuck Dunn, Jim Shufelt, Ed Thierman, and Dresser-Rand test stand personnel. We also thank the Dresser-Rand business, part of Siemens Power & Gas, for allowing us to publish this document.

REFERENCES

Abdelhamid, A.N., 1980, “Analysis of Rotating Stall In Vaneless Diffusers Of Centrifugal Compressors,” ASME Paper No. 80-GT-184.

Abdelhamid, A.N., 1985, “Dynamic Response Of A Centrifugal Blower To Periodic Flow Fluctuations,” ASME Paper No. 85-GT-195.

Abdelhamid, A.N., Betrand, J., 1980, “Distinction Between Two Types Of Self-Excited Gas Oscillations In Vaneless Radial Diffusers,” *Transactions ASME Journal Of Turbomachinery* 109(1): 36-40.

Abdelhamid, A.N., Colwill, W.H., Barrows, J.F., 1979, “Experimental Investigation Of Unsteady Phenomena In Vaneless Radial Diffusers,” ASME Paper No. 78-GT-23, *Transactions ASME Journal Of Engineering For Power* 101(1): 52-60.

Cellai, A., De Lucia, M., Ferrara, G., Ferrari, L., Mengoni, C. P., and Baldassarre, L., 2003, “Application of Low Solidity Vaned Diffusers to Prevent Rotating Stall in Centrifugal Compressors: Experimental Investigation,” ASME Paper No. GT2003-38386.

DeMore, D., Magsoudi, E., Pacheco, J., Sorokes, J., Hutchinson, B., Holmes, W., Lobo, B., Vaibhav, V., 2014, “Investigation of Efficient CFD Methods for Rotating Stall Prediction in a Centrifugal Compressor Stage, “ ASME Paper No. GT2014-27097.

Frigne, P., Van den Braembussche, R., 1984, “Distinctions Between Different Types Of Impeller And Diffuser Rotating Stall In A Centrifugal Compressor With Vaneless Diffuser,” ASME Paper No. 83-GT-61; *Transactions ASME Journal of Engineering Gas Turbine and Power* 106(2): pp. 468-474.

Gourdain, N., Burguburu, S., Leboeuf, F., and Miton, H., 2006, “Numerical Simulation of Rotating Stall in a Subsonic Compressor”, J. of Aerospace Science and Technology, Vol. 10, pp. 9-18.

Izmaylov, R., Lopulalan, H., Norimarna, G., 2012, “Unsteady Flow in Centrifugal Compressor Numerical Modeling and Experimental Investigaion,” ISUAAAT Scientific Committee with JSASS Publication.

Jansen, W., 1964, “Rotating Stall In A Radial Vaneless Diffuser,” ASME Paper No. 64-FE-6, *Transactions ASME Journal of Basic Engineering,* pp. 750-758.

Kobayashi, H., Nishida, H., Takagi, T., Fukushima, Y., 1990, "A Study On The Rotating Stall Of Centrifugal Compressors," (2nd Report, Effect of Vaneless Diffuser Inlet Shape On Rotating Stall) *Transactions Of JSME* (B Edition), 56(529): 98-103.

Ljevar, S., de Lange, H. C., and van Steenhoven, A. A., 2005, "Two-Dimensional Rotating Stall Analysis in a Wide Vaneless Diffuser", International Journal of Rotating Machinery, Vol. 2006, pp. 1-11.

Nishida, H., Kobayashi, H., Takagi, T., Fukushima, Y., 1988, "A Study On The Rotating Stall Of Centrifugal Compressors," (1st Report, Effect Of Vaneless Diffuser Width On Rotating Stall), *Transactions of JSME* 54(499): 589-594.

Senoo, Y., Kinoshita, Y., 1977, "Influence of Inlet Flow Conditions And Geometries Of Centrifugal Vaneless Diffusers On Critical Flow Angles For Reverse Flow," *Transactions ASME Journal of Fluids Engineering*, pp. 98-103.

Senoo, Y., Kinoshita, Y., 1978, "Limits of Rotating Stall And Stall In Vaneless Diffusers Of Centrifugal Compressors," ASME Paper No. 78-GT-19

Senoo, Y., Kinoshita, Y., 1978, Ishida, M., 1977, "Asymmetric Flow In Vaneless Diffusers Of Centrifugal Blowers," *Transactions ASME Journal of Fluids Engineering* 99(1): 104-114.

Sorokes, J. M., Welch, J. P., 1991, "Centrifugal Compressor Performance Enhancement Through The Use Of A Single Stage Development Rig", *Texas A&M Turbomachinery Symposium Proceedings*, pp101-112.

Sorokes, J. M., Welch, J.P., 1992, "Experimental Results on a Rotatable Low Solidity Vaned Diffuser," ASME Paper No. 92-GT-19

Sorokes, J. M., 1993, "The Practical Application OF CFD In The Design Of Industrial Centrifugal Impellers," *Texas A&M Turbomachinery Symposium Proceedings*, pp. 113-124

Sorokes, J. M., 1994, "A CFD Assessment of Entrance Area Distributions in a Centrifugal Compressor Vaneless Diffuser," ASME Paper No. 94-GT-90

Sorokes, J. M., Kuzdzal, M. J., Sandberg, M. R., and Colby, G. M., 1994, "Recent Experiences in Full Load Full Pressure Shop Testing of a High Pressure Gas Injection Centrifugal Compressor," *Texas A&M Turbomachinery Symposium Proceedings*

Vezier C., Dollinger M., Pacheco J. E., Sorokes J., 2013, "Using Unsteady Analysis to Improve the Steady State CFD Assessment of Minimum Flow in a Radial Compressor Stage," ASME paper no. GT2013-95790.

BIBLIOGRAPHY

Bonciani, L., Ferrara, P.L., Timori, A., 1980, "Aero-induced Vibrations In Centrifugal Compressors," *Proceedings of Rotordynamic Instability Problems In High Performance Turbomachinery*, Texas A&M University, NASA CP 2133, pp. 85-94.

Fulton, J.W., 1986, "Subsynchronous Vibration of Multistage Centrifugal Compressors Forced By Rotating Stall," *Proceedings of Rotordynamic Instability Problems In High Performance Turbomachinery*, Texas A&M University.

Japikse, D., 1996, *Centrifugal Compressor Design And Performance*, Concepts ETI, Inc., pp. 5/1 - 5/89.

Kammer, H., Rautenberg, M., 1985, "A Distinction Between Different Types Of Stall In Centrifugal Compressor Stage," ASME Paper No. 85-GT-194

Kushner, F., 1996, "Dynamic Data Analysis of Compressor Rotating Stall," *Texas A&M Turbomachinery Symposium Proceedings*, pp. 71-81.

Kushner, F., Walker, D., and Hohlweg, W., 2002, "Compressor Discharge Pipe Failure Investigation with a Review of Surge, Rotating Stall, and Piping Resonance," *Texas A&M Turbomachinery Symposium Proceedings*, pp. 49-60.

Seidel, U., Chen, J., Jin, D., Rautenberg, M., 1991, "Experimental Investigation Of Rotating Stall Behaviour Influenced By Varying Design And Operation Parameters Of Centrifugal Compressors," Paper No. 91-Yokohama-IGTC-93

Sorokes, J. M., 1995, "Industrial Centrifugal Compressors -- Design Considerations," ASME Paper No. 95-WA/PID-2

Sorokes, J.M., Pacheco, J.E., Vezier, C., and Fakhri, S., 2012, “An Analytical and Experimental Assessment of a Diffuser Flow Phenomenon as a Precursor to Stall”, ASME GT2012-69122.Thomson, W., 1965, *Vibration Theory and Applications*, Prentice-Hall, Inc.

Timoshenko, S., Young, D., and W. Weaver, Jr., 1974, *Vibration Problems in Engineering*, John Wiley & Sons

Volterra, E. and Zachmanoglou, E., 1965, *Dynamics of Vibrations*, Charles E. Merrill Books, Inc.